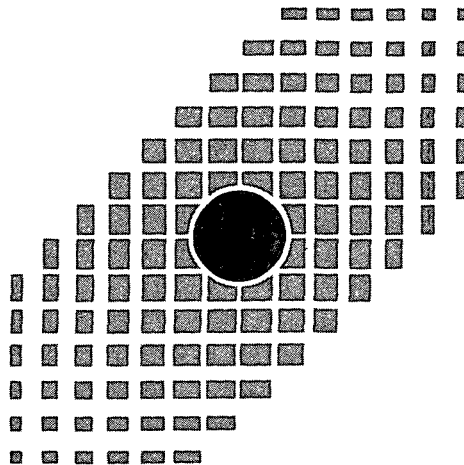


SCHOOL OF ENGINEERING
DUKE UNIVERSITY
DURHAM, NC 27706

**CENTER FOR SOLID-STATE
POWER CONDITIONING
AND CONTROL**



DERIVATION OF LINEARIZED TRANSFER FUNCTIONS
FOR SWITCHING-MODE REGULATORS

PHASE B -- SINGLE-WINDING CURRENT-OR-VOLTAGE STEP-UP
AND TWO-WINDING CURRENT-OR-VOLTAGE STEP-UP CONVERTERS

Prepared by

Ronald C. Wong, Harry A. Owen, Jr., and Thomas G. Wilson

December 15, 1981

for

National Aeronautics and Space Administration
Goddard Space Flight Center

Order No. S-71440B

DERIVATION OF LINEARIZED TRANSFER FUNCTIONS
FOR SWITCHING-MODE REGULATORS
PHASE B -- SINGLE-WINDING CURRENT-OR-VOLTAGE STEP-UP
AND TWO-WINDING CURRENT-OR-VOLTAGE STEP-UP CONVERTERS

Prepared for

National Aeronautics and Space Administration
Goddard Space Flight Center
Greenbelt, Maryland 20771
Order No. S-71440B

Center for Solid-State Power Conditioning and Control
School of Engineering
Duke University
Durham, North Carolina 27706

Ronald C. Wong, Harry A. Owen, Jr., and Thomas G. Wilson
December 15, 1981

1. Report No.	2. Government Accession No.	3. Recipient's Catalog No.	
4. Title and Subtitle Derivation of Linearized Transfer Functions for Switching-Mode Regulators, Phase B -- Single-Winding Current-or-Voltage Step-Up and Two-Winding Current-or-Voltage Step-Up Converters		5. Report Date Dec 15, 1981	
		6. Performing Organization Code	
7. Author(s) R.C. Wong, H.A. Owen, Jr., and T.G. Wilson		8. Performing Organization Report No.	
9. Performing Organization Name and Address Department of Electrical Engineering Duke University Durham, N.C. 27706		10. Work Unit No.	
		11. Contract or Grant No. Order No. S-71440B	
12. Sponsoring Agency Name and Address G.E. Rodriguez, Code 711 Goddard Space Flight Center Greenbelt, Maryland 20771		13. Type of Report and Period Covered	
		14. Sponsoring Agency Code	
15. Supplementary Notes			
16. Abstract <p>Small-signal models are derived for the power stage of the single-winding and two-winding current-or-voltage step-up (buck-boost) converters. The modeling covers operation in both the continuous-mmf mode and the discontinuous-mmf mode.</p>			
17. Key Words (Selected by Author(s)) Small-Signal Models DC-to-DC Converters Continuous-Mmf Mode Discontinuous-Mmf Mode		18. Distribution Statement	
19. Security Classif. (of this report) Unclassified	20. Security Classif. (of this page) Unclassified	21. No. of Pages 91	22. Price*

PREFACE

This Phase B Report documents thoroughly the derivation of a set of small-signal models for the power stages in the single-winding and the two-winding current-or-voltage step-up (buck-boost) energy-storage dc-to-dc converters for operation in both the continuous-mmf mode and the discontinuous-mmf mode. The derivation of the transfer functions describing these power stages is shown in detail and the expressions for the coefficients of these transfer functions are tabulated for ease of application.

TABLE OF CONTENTS

	PAGE
1. INTRODUCTION	1
2. DEVICE MODELS	7
<u>2.1 Transistor Model</u>	7
<u>2.2 Diode Model</u>	10
<u>2.3 Energy-Storage Reactor Model</u>	12
2.3.1 Energy-Storage Reactor Model for the Single-Winding Current-or-Voltage Step-Up (SCVU) Converter	12
2.3.2 Energy-Storage Reactor Model for the Two-Winding Current-or-Voltage Step-Up (TCVU) Converter	14
<u>2.4 Capacitor Model</u>	14
<u>2.5 Load Model</u>	16
3. SOLUTIONS OF STATE VARIABLES IN ONE SWITCHING CYCLE	17
<u>3.1 Description of State Variables in General</u>	19
<u>3.2 Description of State Variables for both SCVU and TCVU</u>	27
4. EQUILIBRIUM OPERATING POINT	32
<u>4.1 Equilibrium Operating Point in the Continuous-Mmf Mode</u>	32
<u>4.2 Equilibrium Operating Point in the Discontinuous-Mmf Mode</u>	38

	PAGE
5. SMALL-SIGNAL TRANSFER FUNCTIONS CHARACTERIZING THE POWER STAGE	45
<u>5.1 Small-Signal Transfer Functions in the Continuous-Mmf Mode</u>	45
<u>5.2 Small-Signal Transfer Functions in the Discontinuous-Mmf Mode</u> ..	65
 6. CLOSED-LOOP FUNCTIONS OF A REGULATED DC-TO-DC CONVERTER	78
<u>6.1 Loop Gain of a Regulated DC-to-DC Converter</u>	78
<u>6.2 Input Impedance of a Regulated DC-to-DC Converter</u>	80
<u>6.3 Audio Susceptibility of a Regulated DC-to-DC Converter</u>	81
<u>6.4 Output Impedance of a Regulated DC-to-DC Converter</u>	81
 7. CONCLUSIONS	82
 8. REFERENCES	83

APPENDICES

	PAGE
A. DEFINITION OF SYMBOLS AND ABBREVIATIONS	84
B. EQUATIONS DEFINING THE CONSTANTS AND THE COEFFICIENTS IN THE TRANSFER FUNCTIONS	86

LIST OF FIGURES

FIGURES	PAGE
1 Block diagram representing the signal flow in a converter power stage	3
2 Steps in arriving at the small-signal closed-loop functions of a regulated dc-to-dc converter	6
3 Piecewise-linear equivalent model of a BJT or FET switch	8
4 Piecewise-linear equivalent model of the diode switch	11
5(a) Model of the energy-storage reactor for the single-winding current-or-voltage step-up converter	13
5(b) Model of the energy-storage reactor for the two-winding current-or-voltage step-up converter with magnetizing inductance L_S referred to the secondary circuit	13
6 Model of the output-filter capacitor	15
7 Model of the power-stage load	15
8(a) Circuit diagram of the power stage of the single-winding current-or-voltage step-up converter	20
8(b) Equivalent model of the power stage shown in 8(a)	20
8(c) Equivalent model of the power stage of the single-winding current-or-voltage step-up converter as obtained from the equivalent circuit shown in Fig. 8(b)	21
9(a) Circuit diagram of the power stage of the two-winding current-or-voltage step-up converter	22
9(b) Equivalent model of the power stage shown in 9(a)	22
9(c) Equivalent model of the power stage of the two-winding current-or-voltage step-up converter as obtained from the equivalent circuit shown in Fig. 9(b)	23
9(d) Equivalent model of the power stage of the two-winding current-or-voltage step-up converter after the primary circuit has been reflected to the secondary circuit	23

FIGURES	PAGE
10	Equivalent circuit of the two-winding current-or-voltage step-up power stage for the three subintervals t_{ON} , t_{OFF1} , and t_{OFF2} 29
11	Interconnection of functional blocks to characterize a converter power stage in the continuous-mmf mode 46
12	Interconnection of functional blocks to characterize a converter power stage in the discontinuous-mmf mode 67
13	Block diagram of a regulated dc-to-dc converter operated from a stiff voltage source 79

LIST OF TABLES

TABLES	PAGE
1 Six Small-Signal Transfer Functions for the Two State Variables Under Continuous-Mmf-Mode Operation 51	51
2 Six Transfer Functions Describing the Load Voltage and the Supply Current for Continuous-Mmf-Mode Operation 62	62
3 Three Transfer Functions for the Ideal Capacitor Voltage Under Discontinuous-Mmf-Mode Operation 69	69
4 Five Transfer Functions Describing the Load Voltage and the Supply Current for Discontinuous-Mmf-Mode Operation 73	73

1. INTRODUCTION

A brief survey of existing approaches to the modeling of switching-mode power systems was presented in Section 1 of the Phase A Report [1] prepared as part of this contract under NASA Order No. S-71440B. In that report, a set of small-signal functions is derived to characterize the voltage step-up (boost) and the current step-up (buck) converters operating under the constant-frequency control law. The basic modeling approach employed in that report starts with the approximation of state transition matrices by second-order Taylor series. From this approximation of the state transition matrices, difference equations for the state variables are developed. Finally, transfer functions are derived to describe the output variables.

Following the same modeling approach employed in the Phase A Report, this Phase B Report documents thoroughly the derivation of a set of small-signal functions for the single-winding and the two-winding current-or-voltage step-up (buck-boost) converters. The equation numbers in this report are assigned the same sequence to match as closely as possible those in the Phase A Report and thereby help the readers to follow the parallel treatment of material common to the two reports. Equations in these two reports can be divided into two groups, those associated with the general modeling approach and those relating to particular converters. Equations relating to the general modeling approach appear identically in these two reports because the same modeling approach is shared between the two. An equation of this type is labeled as (n) where n is the equation number. Equations relating to particular converters, however, differ from converter to converter, depending on the particular converter topology. As a result, an equation relating to a particular converter is labeled as (n,#) where n is the equation number and # is an acronym to identify the particular converter. For example, VU, CU, SCVU, and

TCVU are the acronyms used for the voltage step-up, current step-up, single-winding current-or-voltage step-up, and the two-winding current-or-voltage step-up converters, respectively. Also, there are equations which are common to both the single-winding and the two-winding current-or-voltage step-up converters. Equations of this type are labeled as (n,CVU) where n is the equation number. The tabulation below illustrates the use of the acronyms and the numbering of the equations :

VU	voltage step-up converter
CU	current step-up converter
SCVU	single-winding current-or-voltage step-up converter
TCVU	two-winding current-or-voltage step-up converter
(14)	equation 14, applies to all four converters
(30,VU)	equation 30, applies to the voltage step-up converter
(30,CU)	equation 30, applies to the current step-up converter
(30,CVU)	equation 30, applies to both the single-winding and the two-winding current-or-voltage step-up converters

The symbols used in this report are listed in Appendix A. As far as signal or information flow is concerned, a regulated converter can be represented by the block diagram as shown in Fig. 1. It consists of a dc-to-dc converter power stage with its load, a feedback network, an error detector, and a pulse-width modulator. The power stage is symbolized as having three inputs — the supply voltage v_i , the load-disturbance current i_w , and the duty ratio α_D — and two outputs — the load voltage v_o and the supply current i_i . The feedback network is characterized as a network with the load voltage v_o as its input and feedback voltage v_f as its output. The error detector compares the feedback voltage v_f to the reference voltage v_{REF} and provides an output

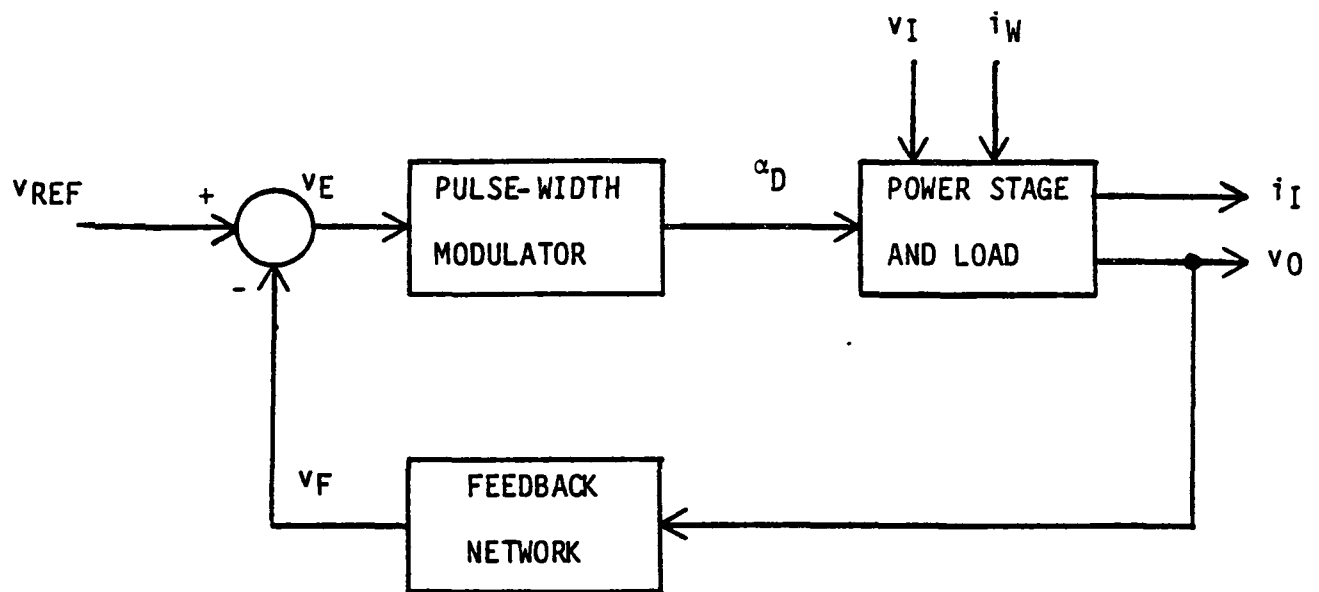


Fig. 1. Block diagram representing the signal flow in a converter power stage.

$v_E = v_F - v_{REF}$. The pulse-width modulator has as its input the error voltage v_E and as its output the duty ratio α_D . The feedback network, the error detector, and the pulse-width modulator often are grouped together into a single functional block called the controller. The signal v_{REF} is a reference-voltage source that establishes the desired dc output voltage V_O .

The first and usually most involved step in characterizing a closed-loop regulated converter under small-signal perturbation conditions is the derivation of the small-signal open-loop functions that describe the power stage of the converter. In deriving these open-loop functions, we need to decide how the various physical devices, such as the energy-storage reactor and the semiconductor switches, are to be modeled in the analysis. We also need information on how the state variables, such as reactor exciting current and output filter-capacitor voltage, vary during one switching period. Determination of the values of the state variables at the beginning of a switching period under equilibrium, i.e., steady-state operating conditions, also is an essential piece of information for deriving these functions.

Section 2 of this report explains how the various physical devices are modeled in this analysis. It also illustrates how the numerical parameters characterizing these models can be obtained. Differential equations for the state variables are set up and solved in Section 3 to describe how the state variables vary during one switching period. Finally, in Section 4, the computation of the equilibrium operating point is illustrated. The various small-signal open-loop functions of the power stage are then derived in Section 5 and expressions for the coefficients of these transfer functions are tabulated.

To completely characterize a closed-loop regulated converter, a model for the controller must be developed. Although there has been some efforts to standardize controller modules [2], the design of a controller is far from unique. It is possible to design a great number of controllers, each achieving the goal of regulating the output voltage of the converter, with vastly different circuitries. These controllers may, or may not, have the same small-signal transfer function. This report does not cover the modeling of controllers. It is assumed that the user can obtain the small-signal transfer function of the controller, either analytically, or experimentally as shown in [3].

Once the power stage and the controller are characterized by their respective small-signal transfer functions, functions such as input impedance, output impedance, and audio susceptibility can be derived for the closed-loop regulated converter. The derivations of such functions are elaborated on in Section 6. The step-by-step procedures to obtain these closed-loop functions are shown in the form of a flow chart in Fig. 2.

REPORT
SECTION NO.

2 {

LOOK UP DEVICE MODELS IN SECTION 2 AND
OBTAIN VARIOUS PARAMETERS FOR THESE MODELS

3 {

COMPUTE THE SIX CONSTANTS IN EQS. (3) TO (8) IN SECTION 3
FOR SCVU, SET $L_S = L$, $r_p = r_S = r_X$, AND $\gamma = 1$

COMPUTE THE APPROXIMATE DUTY RATIO A_D AND INDUCTOR
CURRENT $I_X(kT_S)$ FROM (30,#) AND (31,#)

4 {

CONTINUOUS-MMF MODE

DISCONTINUOUS-MMF MODE

SUBSTITUTE EXISTING VALUE OF
 $I_X(kT_S)$ INTO (32,#) TO SOLVE FOR
 A_D
THEN SUBSTITUTE NEW VALUE OF A_D
INTO (28,#) TO SOLVE FOR $I_X(kT_S)$
ITERATE ON THIS STEP SEVERAL
TIMES

SUBSTITUTE EXISTING VALUE OF
 A_D INTO (38,#) TO SOLVE FOR T_{OFF1}
THEN SUBSTITUTE NEW VALUE OF
 T_{OFF1} INTO (41,#) TO SOLVE FOR A_D
ITERATE ON THIS STEP SEVERAL
TIMES

5 {

LOOK UP TABLES 1 AND 2 AND OBTAIN
THE 12 FUNCTIONS BY COMPUTING
THE CONSTANTS IN (46 a-j,#) AND
(57 a-e,#)

LOOK UP TABLES 3 AND 4 AND OBTAIN
THE 8 FUNCTIONS BY COMPUTING THE
CONSTANTS IN (71,#), (72a-d,#)
(73,#), (62a-d,#), (74,#), AND
(69 a-d,#)

OBTAIN THE TRANSFER FUNCTION OF THE CONTROLLER

6 {

USE BLOCK DIAGRAM IN FIGURE 13 TO
DERIVE DESIRED CLOSED-LOOP FUNCTIONS

END

= CVU

Equations that are mentioned in this flow chart are repeated in Appendix B for quick reference

Fig. 2. Steps in arriving at the small-signal closed-loop functions of a regulated dc-to-dc converter.

2. DEVICE MODELS

In the modeling of the power stage of a dc-to-dc converter, the power transistor, diode, energy-storage reactor, and filter capacitor are replaced with equivalent-circuit models consisting of ideal elements. These equivalent models must be simple enough to make the analysis tractable, while accurate enough to capture the essential features of the devices during the operation of the converter. The device models are presented individually in the following subsections.

2.1 Transistor Model

The power switching transistor is modeled, as shown in Fig. 3, as a series combination of an ideal switch S_Q , a constant voltage V_Q , and a resistor with equivalent resistance r_Q . The switch S_Q is closed when the transistor is switched ON, and it is open when the transistor is switched OFF. The quantity V_Q is equal to the numerical value of the break-point voltage of the transistor in the i_Q versus v_{CE} plane for a bipolar junction transistor (BJT), or in the i_Q versus v_{DS} plane for a field-effect transistor (FET). The value of r_Q' is equal to the differential resistance of the transistor di_Q/dv_Q when it is turned on. The equivalent resistance r_Q in the model, however, is defined in terms of the equivalent resistance needed to account for all of the resistive components of transistor loss, including switching loss, due to the effective value of the transistor current $I_{Q,rms}$. Defining

$$(I_{Q,rms})^2 = \frac{1}{T_S} \int_{T_S} i_Q^2 dt$$

where T_S is the switching period, then r_Q is the required value of resistance such that the product $(I_{Q,rms})^2 r_Q$ corresponds to the total resistive con-

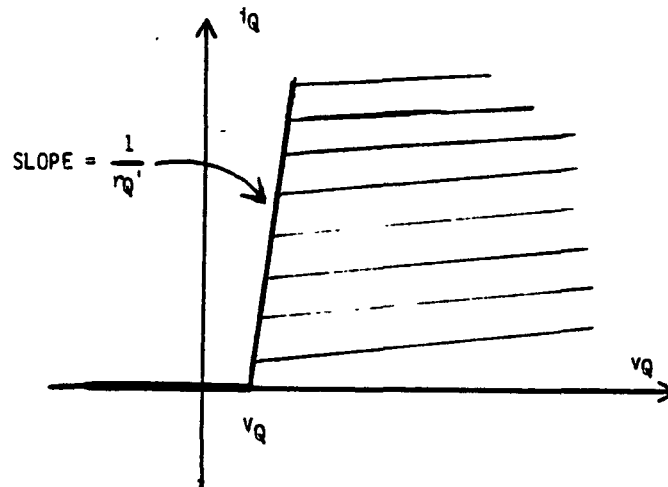
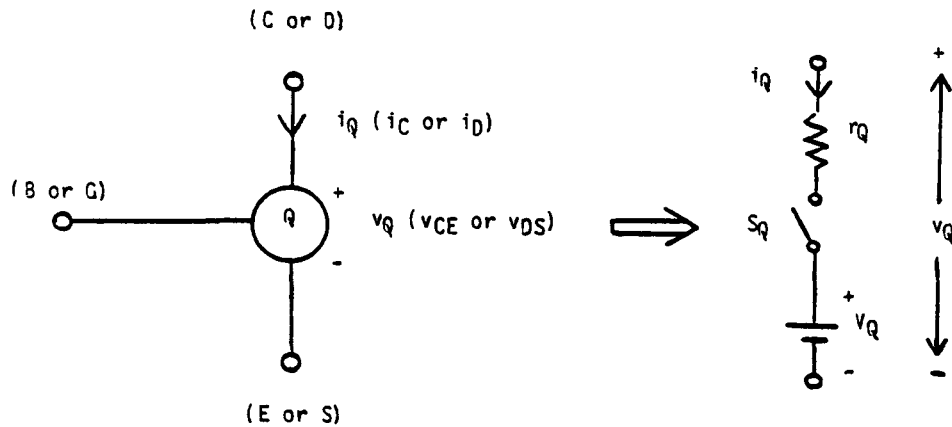


Fig. 3. Piecewise-linear equivalent model of a BJT or an FET switch. For the BJT switch, the base, emitter, and collector terminals are identified by the letters B, E, and C, respectively. For the FET switch, the gate, source, and drain terminals are identified by the letters G, S, and D, respectively.

duction losses, as opposed to the loss due just to the constant component V_Q of the transistor saturation voltage. To find the value of $I_{Q,rms}$ and eventually the value of r_Q , the switching waveforms of the transistor must be determined either by oscillographic measurement or by calculation.

Over one switching cycle of period T_S , the average power loss in the transistor switch is

$$P_Q = \frac{1}{T_S} \int_{T_S} v_Q i_Q dt$$

This power loss P_Q can be viewed as the sum of two components, the loss P_V due to the constant component of the transistor forward drop voltage V_Q when it is conducting, and the remainder of the power loss P_R which can be considered as due to an equivalent resistor r_Q [3]. Therefore,

$$P_V = \frac{1}{T_S} \int_{T_S} V_Q i_Q dt$$

and

$$P_R = P_Q - P_V = \frac{1}{T_S} \int_{T_S} (v_Q - V_Q) i_Q dt$$

Equating P_R to $(I_{Q,rms})^2 r_Q$, we have

$$(I_{Q,rms})^2 r_Q = \frac{1}{T_S} \int_{T_S} (v_Q - V_Q) i_Q dt$$

and the equivalent resistance

$$r_Q = \frac{\int_{T_S} (v_Q - V_Q) i_Q dt}{\int_{T_S} i_Q^2 dt} \quad (1)$$

One possible way of evaluating the integrals shown in (1) is to sample and digitize the actual waveforms of transistor voltage v_Q (v_{CE} or v_{DS}) and current i_Q (i_C or i_D). The digitized results are stored in some storage medium such as the memory registers of a computer or a disk in a computer system. The integration is then performed through numerical summation of the sampled values of $(v_Q - V_Q) i_Q$ and i_Q^2 . This process can be accomplished through the use of a digitizing recorder such as the Biomation 8100 in conjunction with a minicomputer, or through a digital processing oscilloscope such as the Tektronix 7854. If such an instrument is not on hand, one can approximate the switching waveforms with piecewise-linear waveforms. The value of r_Q is then obtained according to (1), with the values of v_Q and i_Q replaced by their piecewise-linear approximations [3].

Where the switching loss is negligible compared to ON-time conduction loss, as for a converter operating at a relatively low switching frequency, r_Q can be approximated by the dynamic resistance r_Q' of the transistor, where r_Q' is defined graphically as shown in Fig. 3.

2.2 Diode Model

In a manner similar to that of the transistor, the diode is modeled as a series combination of an ideal switch S_D , a constant voltage V_D , and a resistor with equivalent resistance r_D . The switch S_D is closed when there is forward current flowing in the physical diode, and it is open otherwise. V_D is equal to the numerical value of the break-point voltage of the diode in the i_D versus v_D plane as shown in Fig. 4. Similar to the definition of r_Q , the equivalent resistance of the diode r_D is defined as

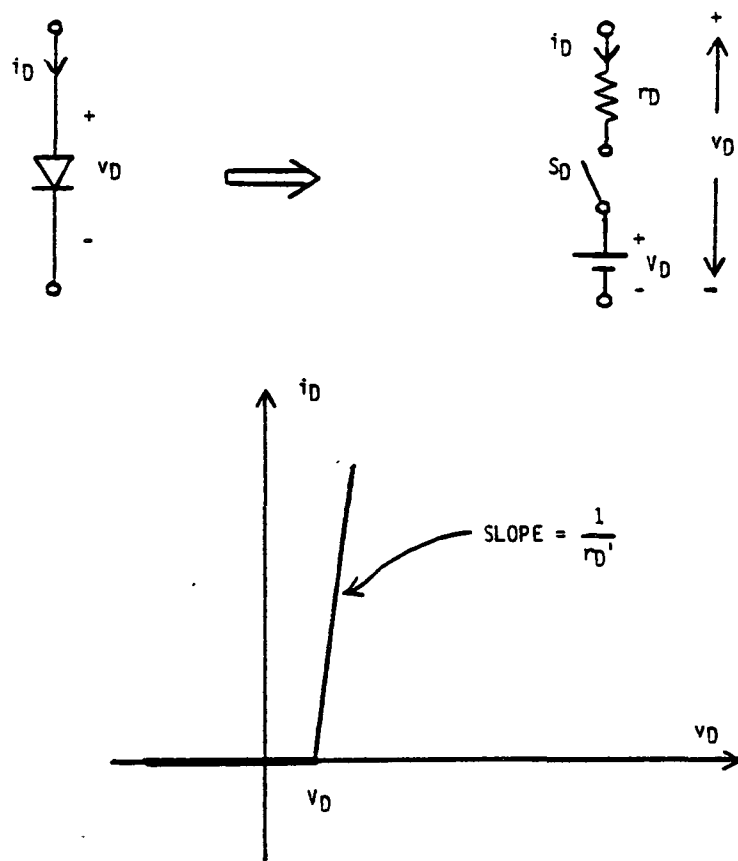


Fig. 4. Piecewise-linear equivalent model of the diode switch.

$$r_D = \frac{\int_{T_S} (v_D - V_D) i_D dt}{\int_{T_S} i_D^2 dt} \quad (2)$$

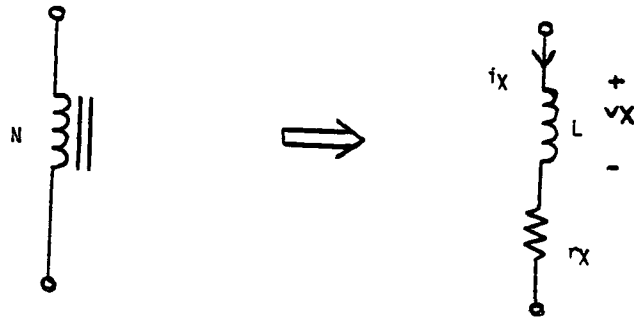
where v_D and i_D are the instantaneous voltage across the diode and the instantaneous current through the diode, respectively. The methods of evaluating integrals outlined in Section 2.1 apply equally well in evaluating the integrals in (2).

In the case where the switching loss is negligible compared to the regular conduction loss, the resistance r_D can be approximated by the dynamic resistance r_D' of the diode, where r_D' is defined graphically in Fig. 4.

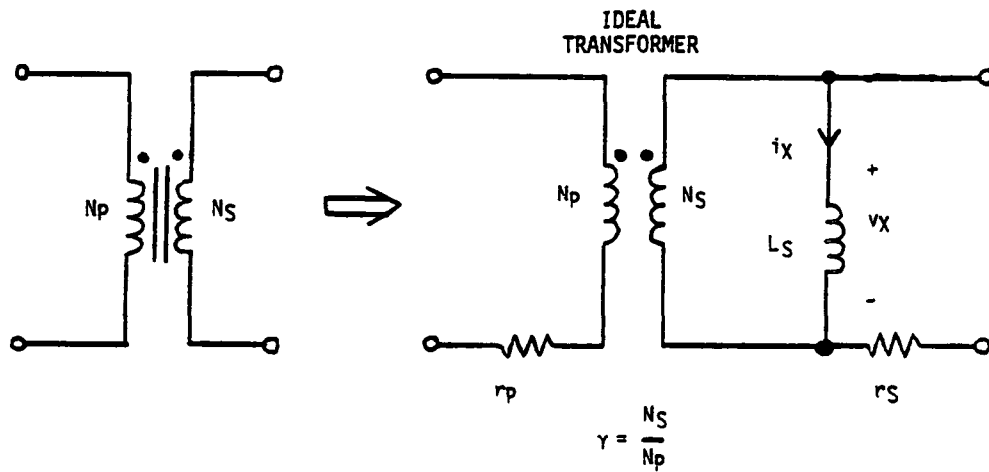
2.3 Energy-Storage Reactor Model

2.3.1 Energy-Storage Reactor Model for the Single-Winding Current-or-Voltage Step-Up (SCVU) converter

The energy-storage reactor for the single-winding current-or-voltage step-up converter (SCVU) is modeled as an ideal inductor L in series with a resistor r_x as shown in Fig. 5(a). Assuming that the reactor core material has a constant permeability, L is then the nominal inductance of the inductor. That is, $L = \mu N^2 A / \ell$, where μ is the absolute permeability of the core material, N is the number of turns, A is the effective cross-sectional area, and ℓ is the mean magnetic path length. The value of resistance for r_x is the winding resistance of the inductor, and it can be estimated when frequency effects can be neglected by finding the wire size of the winding, the number of turns in the winding, and the average length per turn of windings.



(a)



(b)

Fig. 5. (a) Model of the energy-storage reactor for the single-winding current-or-voltage step-up converter. (b) Model of the energy-storage reactor for the two-winding current-or-voltage step-up converter with magnetizing inductance L_s referred to the secondary circuit.

2.3.2 Energy-Storage Reactor Model for the Two-Winding Current-or-Voltage Step-Up (TCVU) Converter

The energy-storage reactor for the two-winding current-or-voltage step-up (TCVU) converter is modeled by a network of linear elements as shown in Fig. 5(b). Neglecting the leakage inductances associated with the primary and secondary windings, the energy-storage reactor is modeled as an ideal transformer with the linear magnetizing inductor L_S connected across the secondary winding. The secondary-to-primary turn ratio of the ideal transformer is equal to $\gamma = N_S/N_p$, the secondary-to-primary turn ratio of the original two-winding reactor. Assuming the core material has a constant permeability, L_S is equal to the nominal inductance of the reactor referred to the secondary winding. That is, $L_S = \mu N_S^2 A / \ell$, where μ is the absolute permeability of the core material, N_S is the number of turns in the secondary winding, A is the effective cross-sectional area and ℓ is the mean magnetic path length. The value of r_p and r_s are the primary and secondary winding resistances, respectively, and they can be estimated in the same way as the estimation of the winding resistance r_x in the single-winding reactor. It is justified to neglect the leakage inductances because they usually result in circuit resonances of frequencies much higher than the switching frequency while the small-signal analysis is valid only in the frequency spectrum below one-half of the switching frequency.

2.4 Capacitor Model

The output filter capacitor of the power stage is modeled as an ideal capacitor C with a voltage of v_C in series with a resistor r_C to represent the equivalent series resistance (ESR) as shown in Fig. 6. The equivalent series inductance (ESL) of the capacitor is ignored because the filter capacitor

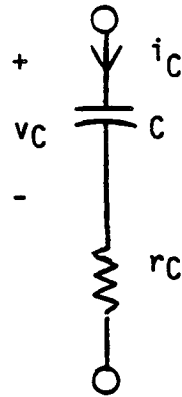


Fig. 6. Model of the output-filter capacitor.

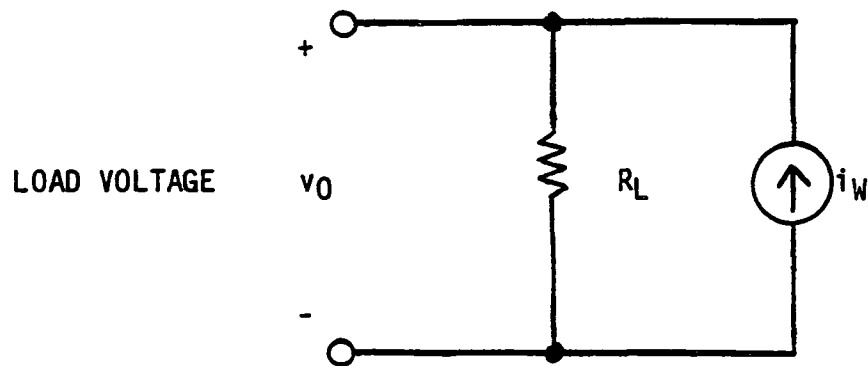


Fig. 7. Model of the power stage load.

employed in a dc-to-dc converter usually is chosen so that its resonant frequency is much higher than the switching frequency f_s , while the small-signal analysis is valid only in the frequency spectrum below one-half of the switching frequency. The value of C is the nominal capacitance of the filter capacitor and r_C can be found by measuring the small-signal impedance of the capacitor at its resonant frequency or from the step jump in capacitor terminal voltage due to an injected step of current through the capacitor.

2.5 Load Model

The converter power-stage load is modeled as an ideal load resistor R_L in parallel with a current source i_W as shown in Fig. 7. The principal purpose of the source i_W is to permit the injection of a disturbance signal at the output port of the converter. Such a signal permits the measurement of the output impedance of the converter and, in such cases, usually is a low-amplitude alternating current. It may, however, also be used to represent the dc equilibrium value of a constant-current component of the total load current.

3. SOLUTIONS OF STATE VARIABLES IN ONE SWITCHING CYCLE

Before going into the description of state variables for the two converter power stages, it is appropriate to explain the convention for the symbols used in this report. For any dynamic variable, such as voltage, current, transistor conduction time, diode conduction time, and duty ratio, the total instantaneous signals are represented by lower-case characters with upper-case subscripts. For example,

Instantaneous values :

Supply voltage	v_I
Duty ratio	α_D
Transistor conduction time	t_{ON}

Each instantaneous signal is assumed to be composed of a dc or equilibrium term and a small-signal variational term. Equilibrium terms are represented by upper-case characters with upper-case subscripts. For example,

Equilibrium values :

Supply voltage	V_I
Duty ratio	A_D
Transistor conduction time	T_{ON}

The small-signal variational terms are represented by lower-case characters with lower-case subscripts. For example,

Variational values:

Supply voltage	v_i
duty ratio	α_d
transistor conduction time	t_{on}

Combining these terms, we have

$$v_I = V_I + v_i$$

$$\alpha_D = A_D + \alpha_d$$

$$t_{ON} = T_{ON} + t_{on}$$

The frequency-domain transformed variables of the small-signal variational terms are represented by upper-case characters with lower-case subscripts. For example,

Frequency-domain variables:

$$V_i(s) = L[v_i(t)]$$

$$A_d(s) = L[\alpha_d(t)]$$

$$T_{on}(s) = L[t_{on}(t)]$$

where s represents the Laplace transform variable and $L[]$ represents the Laplace transformation of the enclosed time function.

Also let us define a set of constants, (3,CVU) to (8,CVU), which facilitate the derivations in the following subsections.

$$\rho = \frac{R_L}{r_C + R_L} \quad (3, CVU)$$

$$\omega_a = \frac{1}{C(r_C + R_L)} \quad (4, CVU)$$

$$\gamma = \frac{N_S}{N_P} \quad (5, CVU)$$

$$\omega_e = \frac{\rho r_C}{L_S} \quad (6, CVU)$$

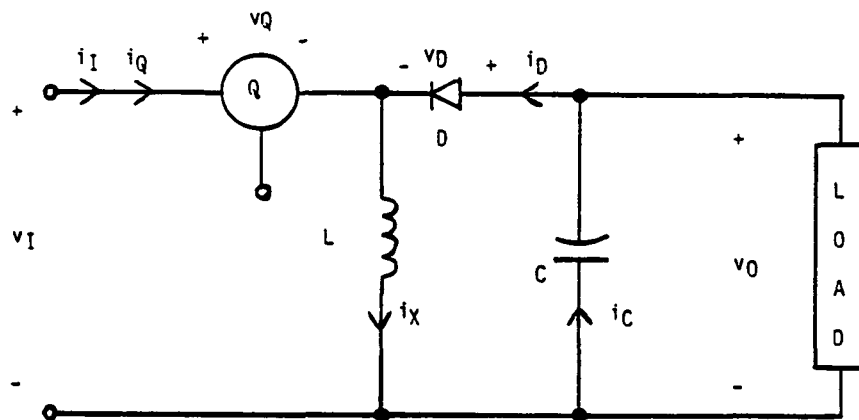
$$\omega_g = \frac{\gamma^2 (r_p + r_q)}{L_S} \quad (7, CVU)$$

$$\omega_h = \frac{r_s + r_D + \rho r_C}{L_S} \quad (8, CVU)$$

3.1 Description of State Variables in General

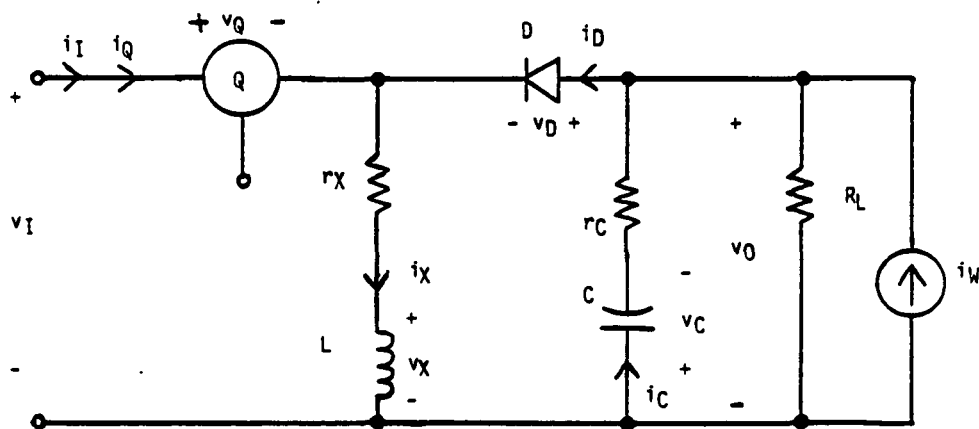
Replacing the energy-storage reactor, the capacitor, and the load with the models derived in Section 2, the power stage of a single-winding current-or-voltage step-up converter shown in Fig. 8(a) can be replaced by an equivalent model in Fig. 8(b). Replacing the transistor and the diode switches with their corresponding models, the circuit shown in Fig. 8(b) is reduced to an equivalent circuit shown in Fig. 8(c). The switch S_Q and S_D in the device models have been combined into one single controllable switch S in Fig. 8(c). Similarly, the power stage of a two-winding current-or-voltage step-up converter shown in Fig. 9(a) is replaced step by step by its equivalent circuits shown in Figs. 9(b) and 9(c). Reflecting the primary circuit of Fig. 9(c) through the ideal transformer to the secondary circuit, the final equivalent circuit shown in Fig. 9(d) is obtained. In Figs. 8(c), 9(c), and 9(d), the switch S assumes position 1 when the transistor is conducting and position 2 when the diode is conducting. If the converter operates in the discontinuous-mode, switch S assumes position 3 for part of the switching cycle when neither the transistor nor the diode conducts.

In general, the converter power stage models in Figs. 8(c) and 9(d) have three controllable input variables — the supply voltage v_I , the load-disturbance current i_W , and the duty ratio α_D , which is defined as the ratio of the time that the transistor is in conduction in one switching cycle t_{ON} to



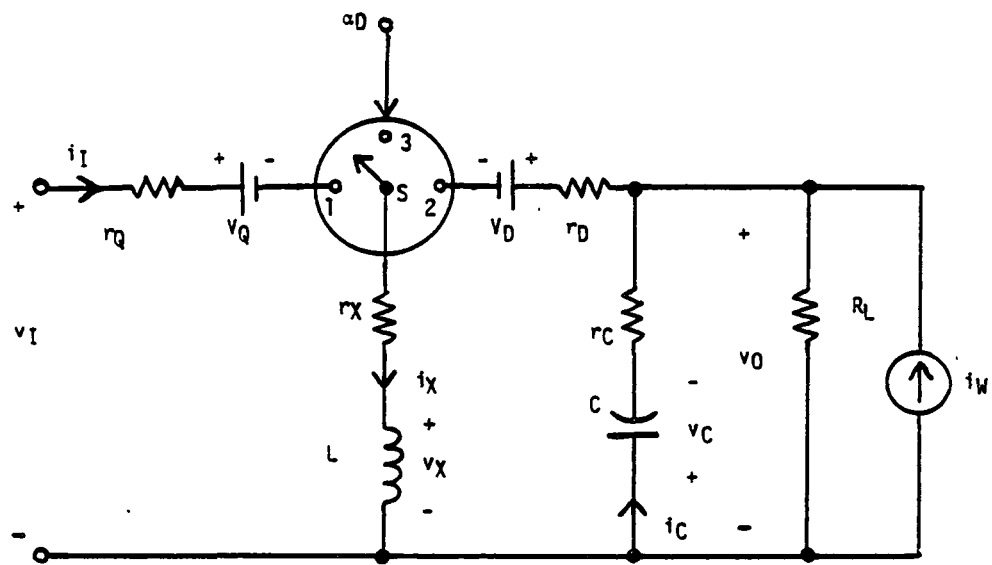
(a)

Fig. 8(a) Circuit diagram of the power stage of the single-winding current-voltage step-up converter.



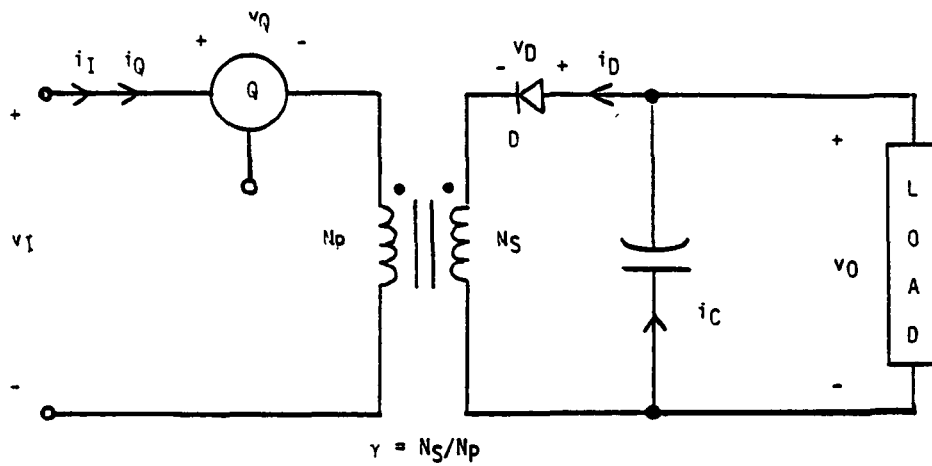
(b)

Fig. 8(b) Equivalent model of the power stage shown in Fig. 8(a).



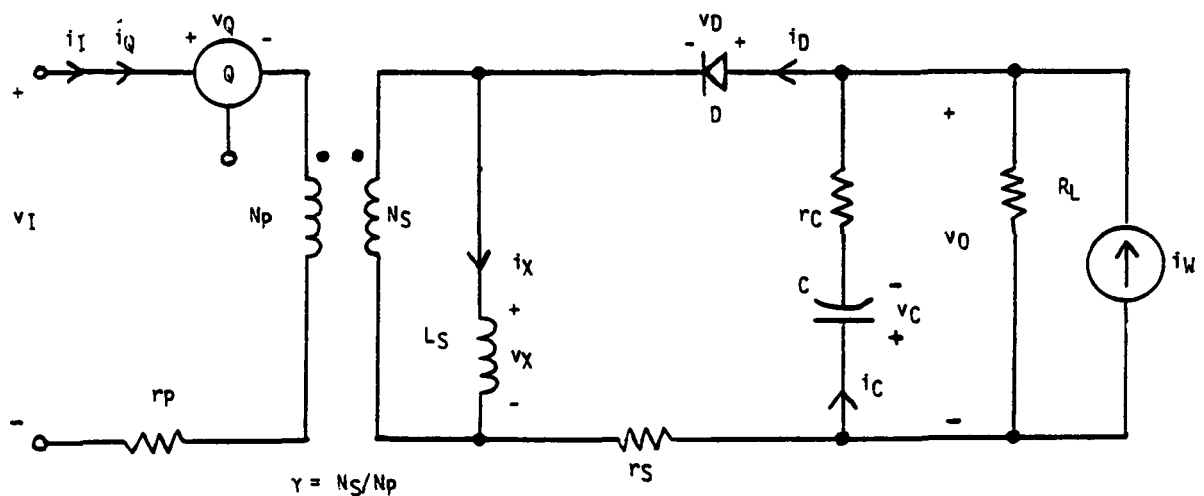
(c)

Fig. 8(c) Equivalent model of the power stage of the single-winding current-voltage step-up converter as obtained from the equivalent circuit shown in Fig. 8(b).



(a)

Fig. 9(a) Circuit diagram of the power stage of the two-winding current-or-voltage step-up converter.



(b)

Fig. 9(b) Equivalent model of the power stage shown in Fig. 9(a).

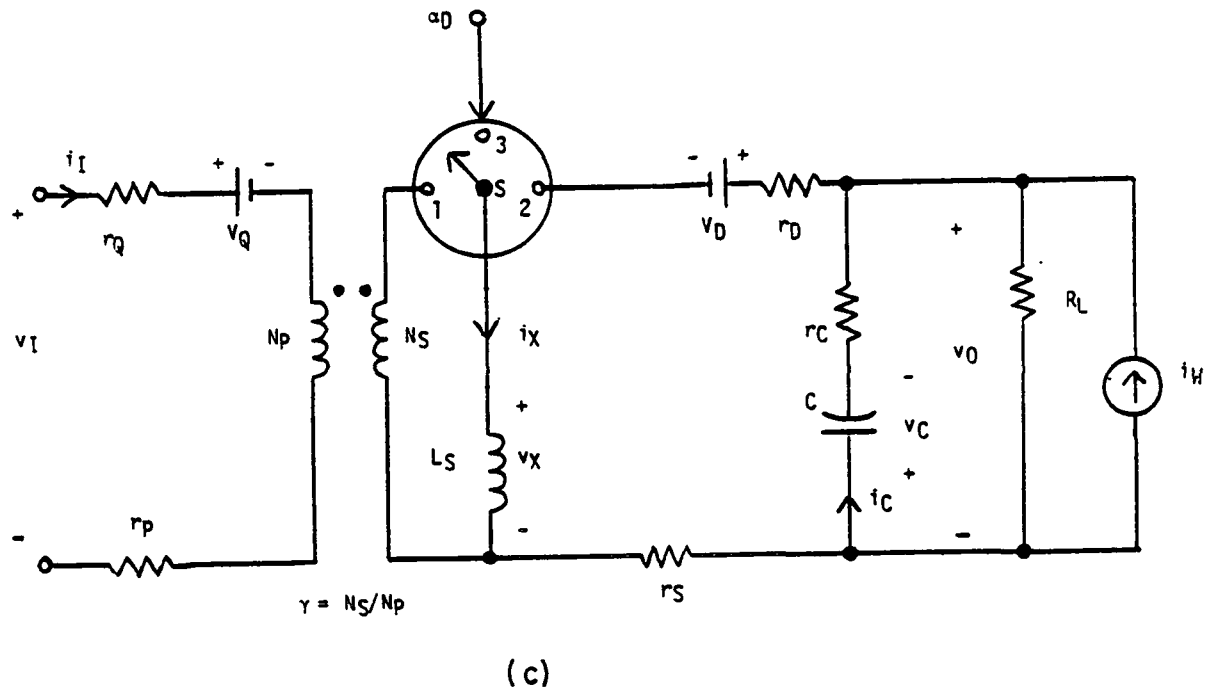


Fig. 9(c) Equivalent model of the power stage of the two-winding current-or-voltage step-up converter as obtained from the equivalent circuit shown in Fig. 9(b).

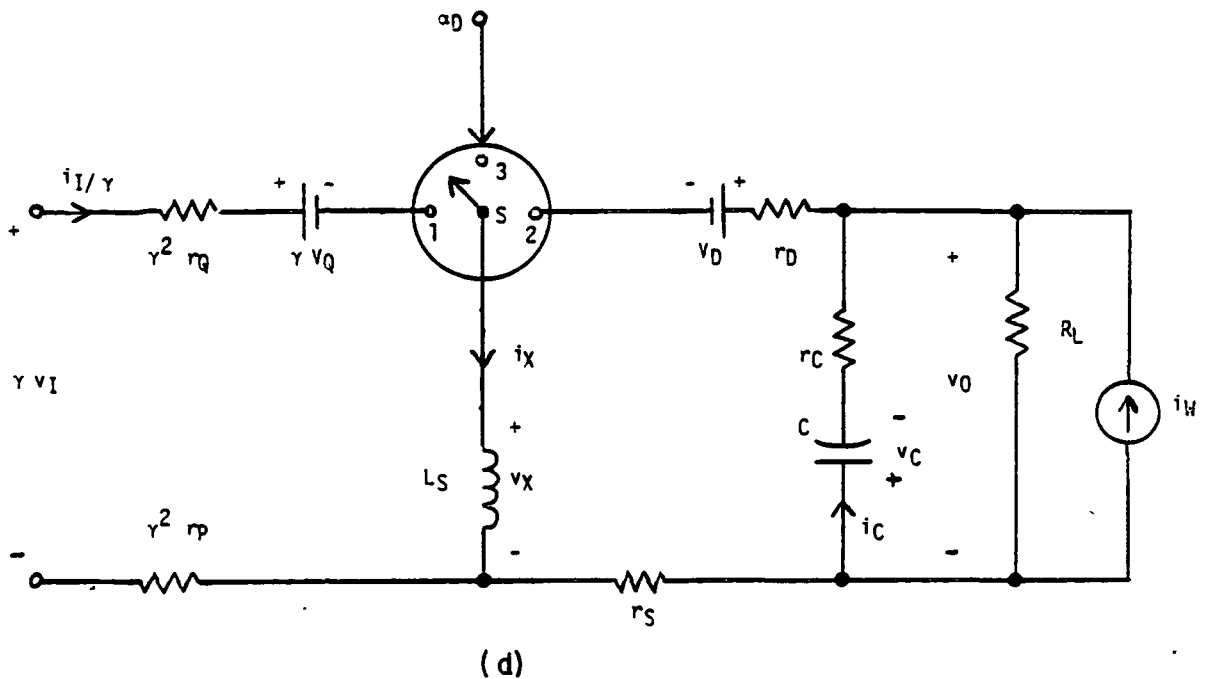


Fig. 9(d) Equivalent model of the power stage of the two-winding current-or-voltage step-up converter after the primary circuit has been reflected to the secondary circuit.

the switching period T_S . There are two state variables — the inductor current i_x and the ideal capacitor voltage v_C . As far as signal flow is concerned, the load voltage v_O and the supply current i_I are looked upon as the response, or the output variables, of the power stage.

The operation of a converter power stage can be classified into two categories: the continuous-mmf mode and the discontinuous-mmf mode. In the continuous-mmf mode, the exciting current i_x of the ideal inductance in the equivalent circuit, L in Fig. 8(c) or L_S in Fig. 9(d), is never equal to zero. As a result, at any time in a switching cycle, either the transistor or the diode is conducting. In the discontinuous-mmf mode, however, the exciting current drops to zero during a certain portion of the switching cycle. Hence, there is an interval during the switching cycle when neither the transistor nor the diode is conducting. Define t_{ON} as the duration of time the transistor conducts in one switching cycle, t_{OFF1} as the duration of time the diode conducts, and t_{OFF2} as the duration of time when neither the transistor nor the diode is conducting. Then, in the continuous-mmf mode,

$$t_{ON} + t_{OFF1} = T_S \quad (9)$$

where T_S is the switching period. In the discontinuous-mmf mode,

$$t_{ON} + t_{OFF1} + t_{OFF2} = T_S \quad (10)$$

Section 3.2 is devoted to setting up the power-stage differential equations in terms of the state variables. The differential equations are then solved, giving a picture of how the state variables vary in one switching cycle.

Whether the converter operates in the continuous- mmf mode or in the discontinuous- mmf mode, in any one of the time intervals t_{ON} , t_{OFF1} , and t_{OFF2} , the power stage state variables satisfy the piecewise-linear differential equations for that interval. This may be expressed for any time interval in compact matrix notation as

$$\frac{d}{dt} \underline{x}_S = \underline{A} \underline{x}_S + \underline{B} \underline{u}_I$$

where \underline{x}_S is the state vector, \underline{u}_I is the input vector, and \underline{A} and \underline{B} are matrices whose elements are topology dependent. Since the circuit topology of the equivalent model of the power stage is altered according to the position of switch S , the matrices \underline{A} and \underline{B} during the time the transistor is conducting usually are different from the \underline{A} and \underline{B} for the case when the diode is conducting. Using the device models established in Section 2, $[v_C \ i_X]^T$ is chosen as the state vector, where T stands for the transpose of matrices and vectors. Likewise, $[v_I \ i_W \ v_Q \ v_D]^T$ is a meaningful choice for the input vector. In terms of these choices, we have

$$\underline{x}_S = [v_C \ i_X]^T \quad (11)$$

$$\underline{u}_I = [v_I \ i_W \ v_Q \ v_D]^T \quad (12)$$

To identify and distinguish relationships that are applicable during the time interval when the transistor is conducting, we attach the subscript ON to the corresponding \underline{A} and \underline{B} matrices. Therefore, during the ON-time in the k th switching cycle for $(kT_S) \leq t \leq (kT_S + t_{\text{ON}})$, where k is an integer,

$$\frac{d}{dt} \underline{x}_S = \underline{A}_{\text{ON}} \underline{x}_S + \underline{B}_{\text{ON}} \underline{u}_I \quad (13)$$

With $\underline{x}_S(kT_S)$ as the initial solution for the vector \underline{x}_S , the general solution to (13) is

$$\underline{x}_S(t) = e^{\underline{A}_{ON}(t-kT_S)} \underline{x}_S(kT_S) + \int_{kT_S}^t e^{\underline{A}_{ON}(t-\tau)} \underline{B}_{ON} \underline{u}_I(\tau) d\tau$$

Assuming \underline{u}_I does not change in one switching cycle, then

$$\begin{aligned} \underline{x}_S(t) &= e^{\underline{A}_{ON}(t-kT_S)} \underline{x}_S(kT_S) + \left[\int_{kT_S}^t e^{\underline{A}_{ON}(t-\tau)} d\tau \right] \underline{B}_{ON} \underline{u}_I \\ &= e^{\underline{A}_{ON}(t-kT_S)} \underline{x}_S(kT_S) - \underline{A}_{ON}^{-1} \left[e^{\underline{A}_{ON}(t-kT_S)} - \underline{I} \right] \underline{B}_{ON} \underline{u}_I \\ &= e^{\underline{A}_{ON}(t-kT_S)} \underline{x}_S(kT_S) + \underline{A}_{ON}^{-1} (e^{\underline{A}_{ON}(t-kT_S)} - \underline{I}) \underline{B}_{ON} \underline{u}_I \end{aligned} \quad (14)$$

where \underline{A}_{ON}^{-1} is the inverse of \underline{A}_{ON} . The assumption that \underline{u}_I does not vary in the switching period is seen to have a far reaching consequence in later sections. This assumption is necessitated by the need to keep the analysis tractable, otherwise the modeling becomes excessively complicated.

During the time interval $(kT_S + t_{ON}) \leq t \leq (kT_S + t_{ON} + t_{OFF1})$, the diode is conducting. Similar to (13), the differential equation in this interval is

$$\frac{d}{dt} \underline{x}_S = \underline{A}_{OFF1} \underline{x}_S + \underline{B}_{OFF1} \underline{u}_I \quad (15)$$

where \underline{A}_{OFF1} and \underline{B}_{OFF1} are matrices whose elements are dependent on the topology and elements in the circuit. Assuming the input vector \underline{u}_I does not change in one switching cycle, then, similar to (14), the solution for the state variables in this interval is

$$\begin{aligned} \underline{x}_S(t) &= e^{\underline{A}_{OFF1}(t-kT_S-t_{ON})} \underline{x}_S(kT_S+t_{ON}) \\ &\quad + \underline{A}_{OFF1}^{-1} (e^{\underline{A}_{OFF1}(t-kT_S-t_{ON})} - \underline{I}) \underline{B}_{OFF1} \underline{u}_I \end{aligned} \quad (16)$$

where $\underline{x}_S(kT_S+t_{ON})$ is the initial condition for this time interval.

If the converter operates in the discontinuous-mmf mode, there will be a third time interval during which neither the transistor nor the diode conducts. Similar to (13) and (15), the differential equation for this interval is

$$\frac{d}{dt} \underline{x}_S = \underline{A}_{OFF2} \underline{x}_S + \underline{B}_{OFF2} \underline{u}_I \quad (17)$$

where \underline{A}_{OFF2} and \underline{B}_{OFF2} are matrices whose elements are dependent on the topology and elements in the circuit. Similar to (14) and (16), the solution for the state variables in this interval is

$$\begin{aligned} \underline{x}_S(t) = & e^{\underline{A}_{OFF2}(t - kT_S - t_{ON} - t_{OFF1})} \underline{x}_S(kT_S + t_{ON} + t_{OFF1}) \\ & + \underline{A}_{OFF2}^{-1} \left(e^{\underline{A}_{OFF2}(t - kT_S - t_{ON} - t_{OFF1})} - \underline{I} \right) \underline{B}_{OFF2} \underline{u}_I \end{aligned} \quad (18)$$

3.2 Description of State Variables for both SCVU and TCVU

An inspection of the equivalent circuits shown in Figs. 8(c) and 9(d) shows that the equivalent circuits of SCVU and TCVU are very similar. In fact, if $\gamma = 1$, $L_S = L$, $r_p = r_x$, and $r_S = r_x$, the equivalent circuit of TCVU shown in Fig. 9(d) is reduced to the equivalent circuit of SCVU shown in Fig. 8(c). Therefore, as far as the description in terms of the state variables is concerned, SCVU is only a special case of TCVU where $\gamma = 1$, $L_S = L$, $r_p = r_x$, and $r_S = r_x$. Starting from this section, equations that are applicable to both SCVU and TCVU are labeled with (n, CVU) where n is the equation number, with the understanding that $\gamma = 1$, $L_S = L$, $r_p = r_x$, and $r_S = r_x$ for the case of SCVU.

In the time interval in which the transistor is conducting, the equivalent model shown in Fig. 9(d) can be reduced further to the circuit shown in

Fig. 10(a). The power-stage differential equations written in terms of the capacitor voltage v_C and the inductor current i_X are :

$$i_C = C \frac{d}{dt} v_C = - \frac{v_C}{r_C + R_L} - \frac{R_L i_W}{r_C + R_L}$$

$$v_X = L_S \frac{d}{dt} i_X = - \gamma^2 (r_p + r_Q) i_X + \gamma v_I - \gamma v_Q$$

Dividing by C throughout the first equation, and by L_S throughout the second one, and substituting symbols defined in (4,CVU) (5,CVU), and (7,CVU)

$$\frac{d}{dt} v_C = -\omega_a v_C - R_L \omega_a i_W$$

$$\frac{d}{dt} i_X = -\omega_g i_X + \frac{\gamma v_I}{L_S} - \frac{\gamma v_Q}{L_S}$$

These two differential equations can be combined to form a single matrix differential equation

$$\frac{d}{dt} \underline{x}_S = \begin{bmatrix} -\omega_a & 0 \\ 0 & -\omega_g \end{bmatrix} \underline{x}_S + \begin{bmatrix} 0 & -R_L \omega_a & 0 & 0 \\ \frac{\gamma}{L_S} & 0 & \frac{-\gamma}{L_S} & 0 \end{bmatrix} \underline{u}_I$$

Comparing the above equation with (13) gives

$$\underline{A}_{ON} = \begin{bmatrix} -\omega_a & 0 \\ 0 & -\omega_g \end{bmatrix} \quad (19, CVU)$$

and

$$\underline{B}_{ON} = \begin{bmatrix} 0 & -R_L \omega_a & 0 & 0 \\ \frac{\gamma}{L_S} & 0 & \frac{-\gamma}{L_S} & 0 \end{bmatrix} \quad (20, CVU)$$

When the initial condition $\underline{x}_S(kT_S)$ is known, the solution for the state variables during this time interval can be obtained by substituting (19,CVU) and (20,CVU) into (14).

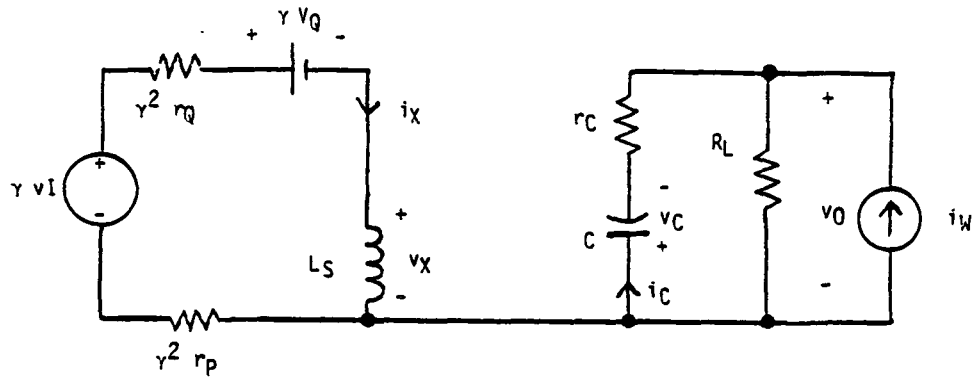
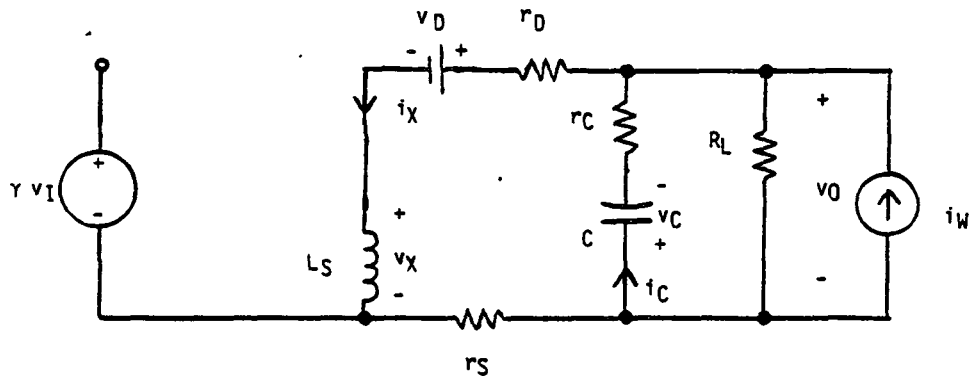
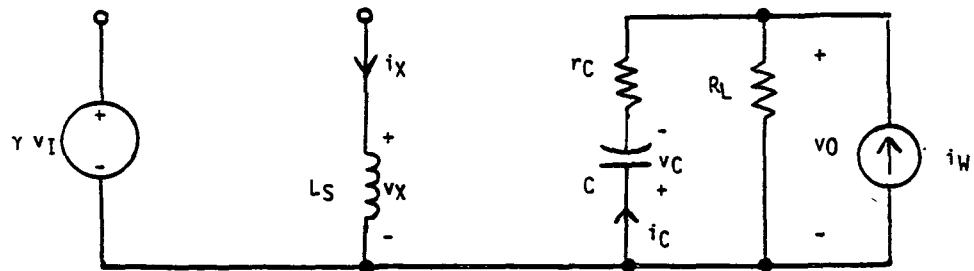
(a) $kT_S \leq t \leq kT_S + t_{ON}$ (b) $kT_S + t_{ON} \leq t \leq kT_S + t_{ON} + t_{OFF1}$ (c) $kT_S + t_{ON} + t_{OFF1} \leq t \leq (k+1)T_S$

Fig. 10. Equivalent circuit of the two-winding current-or-voltage step-up power stage for the three subintervals t_{ON} , t_{OFF1} , and t_{OFF2} .

When switch S in Fig. 9(d) is in position 2, corresponding to conduction of the diode, the equivalent model is reduced to the one shown in Fig. 10(b). From Fig. 10(b), the differential equations are :

$$i_C = C \frac{d}{dt} v_C = - \frac{v_C}{r_C + R_L} + \frac{R_L i_X}{r_C + R_L} - \frac{R_L i_W}{r_C + R_L}$$

$$v_X = L_S \frac{d}{dt} i_X = - \frac{R_L v_C}{r_C + R_L} - \left(r_S + r_D + \frac{r_C R_L}{r_C + R_L} \right) i_X - V_D + \frac{r_C R_L i_W}{r_C + R_L}$$

Dividing the first equation by C, and the second one by L_S , and using the constants defined in (3,CVU), (4,CVU), (6,CVU), and (8,CVU),

$$\frac{d}{dt} v_C = - \omega_a v_C + R_L \omega_a i_X - R_L \omega_a i_W$$

$$\frac{d}{dt} i_X = - \frac{\rho}{L_S} v_C - \omega_h i_X - \frac{V_D}{L_S} + \omega_e i_W$$

which can then be combined into

$$\frac{d}{dt} \underline{x}_S = \begin{bmatrix} -\omega_a & R_L \omega_a \\ \frac{-\rho}{L_S} & -\omega_h \end{bmatrix} \underline{x}_S + \begin{bmatrix} 0 & -R_L \omega_a & 0 & 0 \\ 0 & \omega_e & 0 & \frac{-1}{L_S} \end{bmatrix} \underline{u}_I$$

Comparing the above equation with (15) gives

$$\underline{A}_{OFF1} = \begin{bmatrix} -\omega_a & R_L \omega_a \\ \frac{-\rho}{L_S} & -\omega_h \end{bmatrix} \quad (21, CVU)$$

and

$$\underline{B}_{OFF1} = \begin{bmatrix} 0 & -R_L \omega_a & 0 & 0 \\ 0 & \omega_e & 0 & \frac{-1}{L_S} \end{bmatrix} \quad (22, CVU)$$

When the initial condition $\underline{x}_S(kT_S + t_{ON})$ is known, the solution for the state variables in this time interval can be obtained by substituting (21,CVU) and (22,CVU) into (16).

When switch S in Fig. 9(d) is in position 3, representing the condition that both the transistor and the diode are not conducting, the equivalent model is reduced to the one shown in Fig. 10(c). From Fig. 10(c), the differential equations are :

$$i_C = C \frac{d}{dt} v_C = - \frac{v_C}{r_C + R_L} - \frac{R_L i_W}{r_C + R_L}$$

$$v_X = L_S \frac{d}{dt} i_X = 0$$

Dividing by C throughout the first equation, and using the constant defined in (4,CVU),

$$\frac{d}{dt} \underline{x}_S = \begin{bmatrix} -\omega_a & 0 \\ 0 & 0 \end{bmatrix} \underline{x}_S + \begin{bmatrix} 0 & -R_L \omega_a & 0 & 0 \\ 0 & 0 & 0 & 0 \end{bmatrix} \underline{u}_I$$

Comparing the above equation with (17),

$$\underline{A}_{OFF2} = \begin{bmatrix} -\omega_a & 0 \\ 0 & 0 \end{bmatrix} \quad (23, CVU)$$

and

$$\underline{B}_{OFF2} = \begin{bmatrix} 0 & -R_L \omega_a & 0 & 0 \\ 0 & 0 & 0 & 0 \end{bmatrix} \quad (24, CVU)$$

When the initial condition is known, the solution for the state variables during this time interval can then be obtained by substituting (23,CVU) and (24,CVU) into (18).

4. EQUILIBRIUM OPERATING POINT

4.1 Equilibrium Operating Point in the Continuous-Mmf Mode

In the continuous-mmf mode, the switching period T_S is equal to the sum of the transistor conduction time t_{ON} and the diode conduction time t_{OFF1} . At the end of the k th switching cycle, the time is $t = (k+1)T_S = kT_S + t_{ON} + t_{OFF1}$. At this time, according to (16),

$$\underline{x}_S[(k+1)T_S] = e^{\underline{A}_{OFF1}t_{OFF1}} \underline{x}_S(kT_S + t_{ON}) + \underline{A}_{OFF1}^{-1} (e^{\underline{A}_{OFF1}t_{OFF1}} - \underline{I}) \underline{B}_{OFF1} \underline{u}_I$$

Substituting for $\underline{x}_S(kT_S + t_{ON})$ the value given by (14) evaluated at $t = kT_S + t_{ON}$,

$$\begin{aligned} \underline{x}_S[(k+1)T_S] = & e^{\underline{A}_{OFF1}t_{OFF1}} \{ e^{\underline{A}_{ON}t_{ON}} \underline{x}_S(kT_S) + \underline{A}_{ON}^{-1} (e^{\underline{A}_{ON}t_{ON}} - \underline{I}) \underline{B}_{ON} \underline{u}_I \} \\ & + \underline{A}_{OFF1}^{-1} (e^{\underline{A}_{OFF1}t_{OFF1}} - \underline{I}) \underline{B}_{OFF1} \underline{u}_I \end{aligned}$$

Analogous to the scalar exponential series, the matrix exponential $e^{\underline{M}}$ can be expressed in the series form

$$e^{\underline{M}} = \underline{I} + \frac{\underline{M}}{1!} + \frac{\underline{M}^2}{2!} + \frac{\underline{M}^3}{3!} + \dots$$

for a square matrix \underline{M} . Using the series expansion for the state transition matrices $e^{\underline{A}_{ON}t_{ON}}$ and $e^{\underline{A}_{OFF1}t_{OFF1}}$, and retaining terms only up to second order in T_S , the equation for $\underline{x}_S[(k+1)T_S]$ reduces to

$$\begin{aligned} \underline{x}_S[(k+1)T_S] = & (\underline{I} + \underline{A}_{ON}t_{ON} + \underline{A}_{OFF1}t_{OFF1} + \frac{\underline{A}_{ON}^2 t_{ON}^2 + \underline{A}_{OFF1}^2 t_{OFF1}^2}{2} \\ & + \underline{A}_{OFF1} \underline{A}_{ON} t_{OFF1} t_{ON}) \underline{x}_S(kT_S) \\ & + (\underline{B}_{ON} t_{ON} + \underline{B}_{OFF1} t_{OFF1} + \frac{\underline{A}_{ON} \underline{B}_{ON} t_{ON}^2 + \underline{A}_{OFF1} \underline{B}_{OFF1} t_{OFF1}^2}{2} \\ & + \underline{A}_{OFF1} \underline{B}_{ON} t_{OFF1} t_{ON}) \underline{u}_I \end{aligned} \quad (25)$$

The relationship between the transistor conduction time t_{ON} and the duty ratio α_D is $t_{ON} = \alpha_D T_S$, where T_S is the switching period. Combining $t_{ON} = \alpha_D T_S$ with (9) gives $t_{OFF1} = (1-\alpha_D) T_S$. Now substituting the respective matrices \underline{A}_{ON} , \underline{A}_{OFF1} , \underline{B}_{ON} , and \underline{B}_{OFF1} from (19,CVU) to (22,CVU) into (25), and carrying out the multiplication, the matrix equation can be decomposed into two scalar equations.

$$\begin{aligned}
 v_C[(k+1)T_S] = v_C(kT_S) & \left(1 - \omega_a T_S + \frac{\omega_a^2 T_S^2}{2} - \frac{\rho R_L \omega_a (1-\alpha_D)^2 T_S^2}{2L_S} \right) \\
 & + i_X(kT_S) R_L \omega_a \left((1-\alpha_D) T_S - \omega_g (1-\alpha_D) \alpha_D T_S^2 - \frac{(\omega_a + \omega_h)(1-\alpha_D)^2 T_S^2}{2} \right) \\
 & + \frac{\gamma(V_I - V_Q) R_L \omega_a (1-\alpha_D) \alpha_D T_S^2}{L_S} - \frac{V_D R_L \omega_a (1-\alpha_D)^2 T_S^2}{2L_S} \\
 & - R_L \omega_a i_W \left(T_S - \frac{\omega_a T_S^2}{2} - \frac{\omega_e (1-\alpha_D)^2 T_S^2}{2} \right) \quad (26, CVU)
 \end{aligned}$$

and

$$\begin{aligned}
 i_X[(k+1)T_S] = - \frac{\rho v_C(kT_S)}{L_S} & \left((1-\alpha_D) T_S - \frac{\omega_a (1-\alpha_D^2) T_S^2}{2} - \frac{\omega_h (1-\alpha_D)^2 T_S^2}{2} \right) \\
 & + i_X(kT_S) \left(1 - (\omega_g \alpha_D + \omega_h (1-\alpha_D)) T_S + \frac{(\omega_g \alpha_D + \omega_h (1-\alpha_D))^2 T_S^2}{2} \right. \\
 & \quad \left. - \frac{\rho R_L \omega_a (1-\alpha_D)^2 T_S^2}{2L_S} \right) \\
 & + \frac{\gamma(V_I - V_Q)}{L_S} \left(\alpha_D T_S - \frac{\omega_g \alpha_D^2 T_S^2}{2} - \omega_h (1-\alpha_D) \alpha_D T_S^2 \right) \\
 & + i_W \left(\omega_e (1-\alpha_D) T_S + \frac{\rho R_L \omega_a (1-\alpha_D^2) T_S^2}{2L_S} - \frac{\omega_e \omega_h (1-\alpha_D)^2 T_S^2}{2} \right) \\
 & - \frac{V_D}{L_S} \left((1-\alpha_D) T_S - \frac{\omega_h (1-\alpha_D)^2 T_S^2}{2} \right) \quad (27, CVU)
 \end{aligned}$$

In steady state or equilibrium, all state variables are the same at the end of an arbitrary switching cycle as at the beginning. As a result, using an upper-case character with an upper-case subscript as discussed in the introduction to Section 3 to indicate an equilibrium value, we have $v_C(kT_S) = v_C[(k+1)T_S] = V_C(kT_S)$, $i_X(kT_S) = i_X[(k+1)T_S] = I_X(kT_S)$, $v_I = V_I$, $i_W = I_W$, and $a_D = A_D$. In equilibrium, (26,CVU) and (27,CVU) reduce to

$$\begin{aligned}
 0 = & -\omega_a V_C(kT_S) \left(1 - \frac{\omega_a T_S}{2} + \frac{\rho R_L (1-A_D)^2 T_S}{2L_S} \right) \\
 & + I_X(kT_S) R_L \omega_a (1-A_D) \left(1 - \omega_g A_D T_S - \frac{(\omega_a + \omega_h)(1-A_D) T_S}{2} \right) \\
 & + \frac{\gamma(V_I - V_Q) R_L \omega_a (1-A_D) A_D T_S}{L_S} - \frac{V_D R_L \omega_a (1-A_D)^2 T_S}{2L_S} \\
 & - I_W R_L \omega_a \left(1 - \frac{\omega_a T_S}{2} - \frac{\omega_e (1-A_D)^2 T_S}{2} \right)
 \end{aligned} \tag{28,CVU}$$

and

$$\begin{aligned}
 0 = & -\frac{\rho V_C(kT_S)}{L_S} (1-A_D) \left(1 - \frac{\omega_a (1+A_D) T_S}{2} - \frac{\omega_h (1-A_D) T_S}{2} \right) \\
 & - I_X(kT_S) \left(\omega_g A_D + \omega_h (1-A_D) - \frac{(\omega_g A_D + \omega_h (1-A_D))^2 T_S}{2} + \frac{\rho R_L \omega_a (1-A_D)^2 T_S}{2L_S} \right) \\
 & + \frac{\gamma(V_I - V_Q) A_D}{L_S} \left(1 - \frac{\omega_g A_D T_S}{2} - \omega_h (1-A_D) T_S \right) \\
 & + I_W (1-A_D) \left(\omega_e + \frac{\rho R_L \omega_a (1+A_D) T_S}{2L_S} - \frac{\omega_e \omega_h (1-A_D) T_S}{2} \right) \\
 & - \frac{V_D (1-A_D)}{L_S} \left(1 - \frac{\omega_h (1-A_D) T_S}{2} \right)
 \end{aligned} \tag{29,CVU}$$

Since the converters are designed to provide a constant voltage for the load, the ripple on the ideal capacitor voltage v_C and the load voltage v_0 are usually very small with respect to their corresponding average values. Therefore, the ideal capacitor equilibrium voltage $V_C(kT_S)$ is very close to the value of the specified load voltage V_0 . Hence, $V_C(kT_S)$ can be approximated by the value of V_0 without much loss of accuracy. Once V_I , I_W , V_0 , V_Q , and V_D are specified, the two remaining unknowns $I_X(kT_S)$ and A_D can be computed from (28,CVU) and (29,CVU). The terms T_{ON} and T_{OFF1} are then calculated from the values of A_D and T_S . Equations (28,CVU) and (29,CVU) are linear in $I_X(kT_S)$, but quadratic in A_D . As a result, a closed form solution is not directly accessible. On the other hand, if an approximate solution to A_D and $I_X(kT_S)$ can be found initially, then iteration on (28,CVU) and (29,CVU) can be carried out to obtain more accurate solutions. As a first approximation, all parasitic dissipative elements r_q , r_D , r_p , r_S , and r_C are neglected by assuming they are equal to zero. As a result, ω_a is equal to $1/CR_L$, while ω_e , ω_g , and ω_h are equal to zero, and ρ is equal to one. Equation (29,CVU) is then approximated as

$$0 = \frac{-V_0(1-A_D)}{L_S} \left(1 - \frac{\omega_a(1+A_D)T_S}{2} \right) - \frac{I_X(kT_S)(1-A_D)^2T_S}{2L_SC} + \frac{\gamma(V_I-V_Q)A_D}{L_S} \\ + \frac{I_W(1-A_D^2)T_S}{2L_SC} - \frac{V_D(1-A_D)}{L_S}$$

To maintain a low ripple voltage across the load, the values of L_S and C are usually chosen so that $\omega_a T_S \ll 1$, and $T_S^2/L_SC \ll 1$. Hence, the above equation can be reduced further to

$$\begin{aligned}
 0 &= \frac{-V_0(1-A_D)}{L_S} + \frac{\gamma(V_I-V_Q)A_D}{L_S} - \frac{V_D(1-A_D)}{L_S} \\
 &= A_D (\gamma(V_I-V_Q) + V_0 + V_D) - (V_0 + V_D)
 \end{aligned}$$

which gives

$$A_D = \frac{V_0 + V_D}{\gamma(V_I-V_Q) + V_0 + V_D} \quad (30, CVU)$$

With $\omega_e, \omega_g, \omega_h$ set equal to zero and ρ set equal to one, (28, CVU) can be approximated as

$$\begin{aligned}
 0 &= -\omega_a V_0 \left(1 - \frac{\omega_a T_S}{2} + \frac{R_L(1-A_D)^2 T_S}{2L_S} \right) + I_X(kT_S) R_L \omega_a (1-A_D) \left(1 - \frac{\omega_a (1-A_D) T_S}{2} \right) \\
 &+ \frac{\gamma(V_I-V_Q) R_L \omega_a (1-A_D) A_D T_S}{L_S} - \frac{V_D R_L \omega_a (1-A_D)^2 T_S}{2L_S} \\
 &- I_W R_L \omega_a \left(1 - \frac{\omega_a T_S}{2} \right)
 \end{aligned}$$

Dividing by ω_a and utilizing $\omega_a T_S \ll 1$,

$$\begin{aligned}
 0 &= -V_0 \left(1 + \frac{R_L(1-A_D)^2 T_S}{2L_S} \right) + I_X(kT_S) R_L (1-A_D) \\
 &+ \frac{\gamma(V_I-V_Q) R_L (1-A_D) A_D T_S}{L_S} - \frac{V_D R_L (1-A_D)^2 T_S}{2L_S} - I_W R_L
 \end{aligned}$$

Dividing by $R_L(1-A_D)$, the above equation becomes

$$0 = -\frac{1}{(1-A_D)} \left(\frac{V_0}{R_L} + I_W \right) - \frac{(V_0+V_D)(1-A_D) T_S}{2L_S} + I_X(kT_S) + \frac{\gamma(V_I-V_Q) A_D T_S}{L_S}$$

From (30), $(V_0+V_D)(1-A_D) = \gamma(V_I-V_Q)A_D$, so that

$$0 = - \frac{1}{(1-A_D)} \left(\frac{V_0}{R_L} + I_W \right) + I_X(kT_S) + \frac{\gamma(V_I-V_Q)A_D T_S}{2L_S}$$

$$I_X(kT_S) = \frac{1}{(1-A_D)} \left(\frac{V_0}{R_L} + I_W \right) - \frac{\gamma(V_I-V_Q)A_D T_S}{2L_S} \quad (31, CVU)$$

Most dc-to-dc converters operate with very high efficiency, and the actual values of r_Q , r_D , r_X , and r_C are so small that the equilibrium duty ratio A_D given by (30, CVU) and the equilibrium inductor current $I_X(kT_S)$ given by (31, CVU) are within one to two percent of the values obtained from experimental measurements. If these dissipative elements are large enough to affect significantly the values of A_D and $I_X(kT_S)$, the operating point can be located by using iterative methods. Equation (29, CVU) can be rewritten as a quadratic in A_D :

$$0 = A_D^2 T_S \left\{ \frac{\rho(\omega_I - \omega_a)V_0}{2L_S} - \frac{I_X(kT_S)}{2} \left(\frac{\rho R_L \omega_a}{L_S} - (\omega_g - \omega_h)^2 \right) \right. \\ \left. - \frac{I_W}{2} \left(\frac{\rho R_L \omega_a}{L_S} + \omega_e \omega_h \right) - \frac{\gamma(V_I - V_Q)(\omega_g - 2\omega_h)}{2L_S} + \frac{V_D \omega_h}{2L_S} \right\} \\ + A_D \left\{ (1 - \omega_h T_S) \left(\frac{\rho V_0 + V_D + \gamma(V_I - V_Q)}{L_S} - \omega_e I_W + (\omega_I - \omega_g) I_X(kT_S) \right) \right. \\ \left. + \frac{I_X(kT_S) \rho R_L \omega_a T_S}{L_S} \right\} \\ + \left\{ \frac{(2 - \omega_h T_S)}{2} \left(- \frac{V_D + \rho V_0}{L_S} - \omega_h I_X(kT_S) + \omega_e I_W \right) \right. \\ \left. + \frac{\rho \omega_a T_S (V_0 - R_L I_X(kT_S) + R_L I_W)}{2L_S} \right\} \quad (32, CVU)$$

First, substitute the specified constants V_I , V_0 , V_Q , V_D , and I_W , and the constants ρ , ω_a , ω_e , ω_g , and ω_h into (32, CVU) and (28, CVU). Then substitute the

approximation for $I_X(kT_S)$ from (31,CVU) into (32,CVU) and solve for a new solution for A_D . Substituting the new A_D into (28,CVU), a better approximation for $I_X(kT_S)$ can be computed. The new value for $I_X(kT_S)$ can then be substituted into (32,CVU) to obtain a more accurate value for A_D . Working back and forth between (32,CVU) and (28,CVU) once or twice will give highly accurate solutions for the equilibrium duty ratio A_D and the equilibrium inductor current $I_X(kT_S)$.

4.2 Equilibrium Operating Point in the Discontinuous-Mmf Mode

In the discontinuous-mmf mode, the inductor current is always equal to zero at the beginning of each switching cycle, that is, $i_X(kT_S) = i_X[(k+1)T_S] = 0$. Also, $t_{OFF2} = T_S - t_{ON} - t_{OFF1}$. Evaluating (18) at $t = (k+1)T_S$,

$$\begin{aligned} \underline{x}_S[(k+1)T_S] &= e^{\underline{A}_{OFF2}(T_S - t_{ON} - t_{OFF1})} \underline{x}_S(kT_S + t_{ON} + t_{OFF1}) \\ &\quad + \underline{A}_{OFF2}^{-1} \left(e^{\underline{A}_{OFF2}(T_S - t_{ON} - t_{OFF1})} - \underline{I} \right) \underline{B}_{OFF2} \underline{u}_I \end{aligned}$$

Evaluating (14) at $t = kT_S + t_{ON}$ and (16) at $t = kT_S + t_{ON} + t_{OFF1}$,

$$\underline{x}_S(kT_S + t_{ON}) = e^{\underline{A}_{ON}t_{ON}} \underline{x}_S(kT_S) + \underline{A}_{ON}^{-1} \left(e^{\underline{A}_{ON}t_{ON}} - \underline{I} \right) \underline{B}_{ON} \underline{u}_I$$

and

$$\begin{aligned} \underline{x}_S(kT_S + t_{ON} + t_{OFF1}) &= e^{\underline{A}_{OFF1}t_{OFF1}} \underline{x}_S(kT_S + t_{ON}) \\ &\quad + \underline{A}_{OFF1}^{-1} \left(e^{\underline{A}_{OFF1}t_{OFF1}} - \underline{I} \right) \underline{B}_{OFF1} \underline{u}_I \end{aligned}$$

Combining the three equations above gives

$$\begin{aligned}
\underline{x}_S[(k+1)T_S] = & e^{\underline{A}_{OFF2}(T_S - t_{ON} - t_{OFF1})} \left\{ e^{\underline{A}_{OFF1} t_{OFF1}} \left[e^{\underline{A}_{ON} t_{ON}} \underline{x}_S(kT_S) \right. \right. \\
& + \underline{A}_{ON}^{-1} \left(e^{\underline{A}_{ON} t_{ON}} - \underline{I} \right) \underline{B}_{ON} \underline{u}_I \left. \right] \\
& + \underline{A}_{OFF1}^{-1} \left(e^{\underline{A}_{OFF1} t_{OFF1}} - \underline{I} \right) \underline{B}_{OFF1} \underline{u}_I \left. \right\} \\
& + \underline{A}_{OFF2}^{-1} \left(e^{\underline{A}_{OFF2}(T_S - t_{ON} - t_{OFF1})} - \underline{I} \right) \underline{B}_{OFF2} \underline{u}_I
\end{aligned}$$

Expanding the state transition matrices $e^{\underline{A}_{ON} t_{ON}}$, $e^{\underline{A}_{OFF1} t_{OFF1}}$, and $e^{\underline{A}_{OFF2}(T_S - t_{ON} - t_{OFF1})}$ into a set of power series, and retaining terms only up to second order in T_S ,

$$\begin{aligned}
\underline{x}_S[(k+1)T_S] = & \left\{ \underline{I} + \underline{A}_{ON} t_{ON} + \underline{A}_{OFF1} t_{OFF1} + \underline{A}_{OFF2}(T_S - t_{ON} - t_{OFF1}) \right. \\
& + \frac{\underline{A}_{ON}^2 t_{ON}^2 + \underline{A}_{OFF1}^2 t_{OFF1}^2 + \underline{A}_{OFF2}^2 (T_S - t_{ON} - t_{OFF1})^2}{2} \\
& + \underline{A}_{OFF1} \underline{A}_{ON} t_{OFF1} t_{ON} + \underline{A}_{OFF2} \underline{A}_{ON} (T_S - t_{ON} - t_{OFF1}) t_{ON} \\
& \left. + \underline{A}_{OFF2} \underline{A}_{OFF1} (T_S - t_{ON} - t_{OFF1}) t_{OFF1} \right\} \underline{x}_S(kT_S) \\
& + \left\{ \underline{B}_{ON} t_{ON} + \underline{B}_{OFF1} t_{OFF1} + \underline{B}_{OFF2}(T_S - t_{ON} - t_{OFF1}) \right. \\
& + \frac{\underline{A}_{ON} \underline{B}_{ON} t_{ON}^2 + \underline{A}_{OFF1} \underline{B}_{OFF1} t_{OFF1}^2 + \underline{A}_{OFF2} \underline{B}_{OFF2} (T_S - t_{ON} - t_{OFF1})^2}{2} \\
& + \underline{A}_{OFF1} \underline{B}_{ON} t_{OFF1} t_{ON} + \underline{A}_{OFF2} \underline{B}_{ON} (T_S - t_{ON} - t_{OFF1}) t_{ON} \\
& \left. + \underline{A}_{OFF2} \underline{B}_{OFF1} (T_S - t_{ON} - t_{OFF1}) t_{OFF1} \right\} \underline{u}_I
\end{aligned} \tag{33}$$

Substituting the respective matrices \underline{A}_{ON} , \underline{A}_{OFF1} , \underline{A}_{OFF2} , \underline{B}_{ON} , \underline{B}_{OFF1} , and \underline{B}_{OFF2} from (19,CVU) to (24,CVU) into (33) and carrying out the multiplication, the matrix equation can be decomposed into two scalar equations.

$$\begin{aligned}
 v_C[(k+1)T_S] = & v_C(kT_S) \left(1 - \omega_a T_S + \frac{\omega_a^2 T_S^2}{2} - \frac{\rho R_L \omega_a t_{OFF1}^2}{2L_S} \right) \\
 & + \frac{\gamma (V_I - V_Q) R_L \omega_a t_{OFF1} t_{ON}}{L_S} - \frac{V_D R_L \omega_a t_{OFF1}^2}{2L_S} \\
 & - R_L \omega_a i_W \left(T_S - \frac{\omega_a T_S^2}{2} - \frac{\omega_e t_{OFF1}^2}{2} \right) \quad (34, CVU)
 \end{aligned}$$

and

$$\begin{aligned}
 0 = & - \frac{\rho v_C(kT_S)}{L_S} \left(t_{OFF1} - \frac{\omega_h t_{OFF1}^2}{2} - \frac{\omega_a t_{OFF1}}{2} (t_{OFF1} + 2t_{ON}) \right) \\
 & + \frac{\gamma (V_I - V_Q)}{L_S} \left(t_{ON} - \frac{\omega_g t_{ON}^2}{2} - \omega_h t_{OFF1} t_{ON} \right) - \frac{V_D}{L_S} \left(t_{OFF1} - \frac{\omega_h t_{OFF1}^2}{2} \right) \\
 & + i_W \left(\omega_e t_{OFF1} - \frac{1}{2}(\omega_e \omega_h - \frac{\rho R_L \omega_a}{L_S}) t_{OFF1}^2 + \frac{\rho R_L \omega_a t_{OFF1} t_{ON}}{L_S} \right) \quad (35, CVU)
 \end{aligned}$$

The identity $i_X(kT_S) = i_X[(k+1)T_S] = 0$ has been used in deriving these two equations. For (35,CVU), terms in powers of t_{OFF1} can be grouped to obtain

$$\begin{aligned}
 0 = & t_{OFF1}^2 \left(\frac{\rho \omega_a (v_C(kT_S) + R_L i_W)}{2L_S} + \frac{\omega_h (\rho v_C(kT_S) + V_D)}{2L_S} - \frac{\omega_e \omega_h i_W}{2} \right) \\
 & + t_{OFF1} \left(\frac{\rho \omega_a t_{ON} (v_C(kT_S) + R_L i_W)}{L_S} - \frac{\gamma (V_I - V_Q) \omega_h t_{ON}}{L_S} + \omega_e i_W - \frac{\rho v_C(kT_S) + V_D}{L_S} \right) \\
 & + \left(\frac{\gamma (V_I - V_Q) t_{ON} (2 - \omega_g t_{ON})}{2L_S} \right) \quad (36, CVU)
 \end{aligned}$$

Equations (34,CVU) to (36,CVU) are equations based on the piecewise-linear description of the instantaneous values of the state variables over one complete steady-state cycle. In steady state or equilibrium, all state variables are the same at the end of an arbitrary switching cycle as at the beginning. As a result, using an upper-case character with an upper-case subscript as discussed in the introduction to Section 3 to indicate an equilibrium value, we have $v_C(kT_S) = v_C[(k+1)T_S] = V_C(kT_S)$, $v_I = V_I$, and $i_W = I_W$. Since a stringent restriction on the ripple of the load voltage is usually placed on a dc-to-dc converter, the ideal capacitor equilibrium voltage $V_C(kT_S)$ is very close to the load voltage V_O . Hence, $V_C(kT_S)$ can be approximated by the value of V_O without much degradation of accuracy. Thus, under steady-state or equilibrium, (34,CVU) and (36,CVU) reduce to

$$0 = -\omega_a V_O \left(T_S - \frac{\omega_a T_S^2}{2} + \frac{\rho R_L T_{OFF1}^2}{2L_S} \right) + \frac{\gamma R_L \omega_a (V_I - V_Q) T_{OFF1} T_{ON}}{L_S} \\ - R_L \omega_a I_W \left(T_S - \frac{\omega_a T_S^2}{2} - \frac{\omega_e T_{OFF1}^2}{2} \right) - \frac{R_L \omega_a V_D T_{OFF1}^2}{2L_S} \quad (37, CVU)$$

and

$$0 = T_{OFF1}^2 \left(\frac{\rho \omega_a (V_O + R_L I_W)}{2L_S} + \frac{\omega_h (\rho V_O + V_D)}{2L_S} - \frac{\omega_e \omega_h I_W}{2} \right) \\ + T_{OFF1} \left(\frac{\rho \omega_a T_{ON} (V_O + R_L I_W)}{L_S} - \frac{\gamma (V_I - V_Q) \omega_h T_{ON}}{L_S} - \frac{\rho V_O + V_D}{L_S} + \omega_e I_W \right) \\ + \left(\frac{\gamma (V_I - V_Q) T_{ON} (2 - \omega_g T_{ON})}{2L_S} \right) \quad (38, CVU)$$

For specified supply voltage, load voltage, and load, the two unknowns in the steady-state analysis of a converter operating in the continuous-mmf mode are the duty ratio A_D and the inductor current $I_X(kT_S)$. The diode conduction time T_{OFF1} is simply defined by $T_{OFF1} = T_S(1 - A_D)$. On the other hand, for specified supply voltage, load voltage, and load, the two unknowns in the steady-state analysis of a converter operating in the discontinuous-mmf mode are the duty ratio A_D and the diode conduction time T_{OFF1} . The value of $I_X(kT_S)$, however, is always equal to zero in the case of the discontinuous-mmf mode. The values of the two unknowns A_D and T_{OFF1} can be obtained from the two simultaneous equations (37,CVU) and (38,CVU). First, approximations to A_D and T_{OFF1} are found by neglecting the parasitic dissipative elements r_q , r_D , r_p , r_S , and r_C . As a consequence, with ω_a equal to $1/CR_L$, ω_e , ω_g , and ω_h equal to zero, and ρ equal to one, (38,CVU) is reduced to

$$0 = T_{OFF1}^2 \left(\frac{V_0 + R_L I_W}{2R_L L_S C} \right) + T_{OFF1} \left(\frac{T_{ON}(V_0 + R_L I_W)}{R_L L_S C} - \frac{V_0 + V_D}{L_S} \right) + \left(\frac{\gamma(V_I - V_Q)T_{ON}}{L_S} \right)$$

Since T_{OFF1} is of the order T_S , and T_{ON} is also of the order T_S , the use of the inequalities $\omega_a T_S \ll 1$ and $T_S^2/LC \ll 1$ reduces the above equation to

$$0 = - \frac{T_{OFF1}(V_0 + V_D)}{L_S} + \frac{\gamma(V_I - V_Q)T_{ON}}{L_S}$$

or

$$T_{OFF1} = \frac{\gamma(V_I - V_Q)T_{ON}}{V_0 + V_D} = \frac{\gamma(V_I - V_Q)A_D T_S}{V_0 + V_D} \quad (39, CVU)$$

Although (39,CVU) gives T_{OFF1} as a function of A_D , V_I , V_0 , V_Q , and V_D , the equilibrium duty ratio A_D is still unknown at this moment. With ω_e , ω_g , and ω_h equal to zero and ρ equal to one, (37,CVU) reduces to

$$0 = -\omega_a T_S V_0 \left(1 - \frac{\omega_a T_S}{2} + \frac{R_L T_{OFF1}^2}{2L_S T_S} \right) + \frac{\gamma R_L \omega_a T_S (V_I - V_Q) T_{OFF1} A_D}{L_S} \\ - R_L \omega_a T_S I_W \left(1 - \frac{\omega_a T_S}{2} \right) - \frac{R_L \omega_a T_S V_D T_{OFF1}^2}{2L_S T_S}$$

Dividing the above equation by $\omega_a T_S$, and noting that $\omega_a T_S$ is negligible when compared to unity,

$$0 = -V_0 \left(1 + \frac{R_L T_{OFF1}^2}{2L_S T_S} \right) + \frac{\gamma R_L (V_I - V_Q) T_{OFF1} A_D}{L_S} - R_L I_W - \frac{R_L V_D T_{OFF1}^2}{2L_S T_S} \\ = -V_0 - R_L I_W + \frac{\gamma (V_I - V_Q) R_L T_{OFF1} A_D}{L_S} - \frac{(V_0 + V_D) R_L T_{OFF1}^2}{2L_S T_S}$$

which then leads to

$$V_0 + R_L I_W = \frac{\gamma (V_I - V_Q) R_L T_{OFF1} A_D}{L_S} - \frac{(V_0 + V_D) R_L T_{OFF1}^2}{2L_S T_S}$$

Substituting the expression for T_{OFF1} from (39,CVU) into the above equation,

$$V_0 + R_L I_W = \frac{\gamma^2 (V_I - V_Q)^2 R_L A_D^2 T_S}{L_S (V_0 + V_D)} - \frac{\gamma^2 (V_I - V_Q)^2 R_L A_D^2 T_S}{2L_S (V_0 + V_D)} \\ = \frac{\gamma^2 (V_I - V_Q)^2 R_L A_D^2 T_S}{2L_S (V_0 + V_D)}$$

giving

$$A_D = \sqrt{\frac{2L_S (V_0 + R_L I_W) (V_0 + V_D)}{\gamma^2 R_L T_S (V_I - V_Q)^2}} \quad (40, CVU)$$

If the solutions for A_D and T_{OFF1} given by (40,CVU) and (39,CVU) are not accurate enough, more accurate solutions can be obtained through iterative procedures. Dividing (37,CVU) by $\omega_a T_S$, and rewriting it,

$$0 = A_D \left(\frac{\gamma(V_I - V_Q) R_L T_{OFF1}}{L_S} \right) + \left\{ -V_0 \left(1 - \frac{\omega_a T_S}{2} + \frac{\rho R_L T_{OFF1}^2}{2 L_S T_S} \right) - \frac{V_D R_L T_{OFF1}^2}{2 L_S T_S} - R_L I_W \left(1 - \frac{\omega_a T_S}{2} - \frac{\omega_e T_{OFF1}^2}{2 T_S} \right) \right\} \quad (41, CVU)$$

Now substitute the specified V_I , V_Q , V_D , and I_W , and the constants ρ , ω_a , ω_e , ω_g , and ω_h into (38, CVU) and (41, CVU). Substitute $T_{ON} = A_D T_S$, where A_D is obtained from (40, CVU) into (38, CVU) and solve for a new value for T_{OFF1} . Then substitute the new T_{OFF1} into (41, CVU) and obtain a more accurate approximation on A_D . Working back and forth between (38, CVU) and (41, CVU) once or twice will give highly accurate solutions for the equilibrium point.

5. SMALL-SIGNAL TRANSFER FUNCTIONS CHARACTERIZING THE POWER STAGE

5.1 Small-Signal Transfer Functions in the Continuous-Mmf Mode

As outlined in Section 3.1, the signal flow of the power stage of a dc-to-dc converter may be modeled as a network with three controllable input variables, the duty ratio α_D , the supply voltage v_I , and the load-disturbance current i_W ; two state variables, the capacitor voltage v_C and the inductor current i_X ; and two output variables, the load voltage v_O and the supply current i_I . In order to model the power stage, including its load, in the small-signal frequency domain, transfer functions relating the input variables, the state variables, and the output variables have to be derived. Figure 11 shows a block diagram representing the power stage and the twelve transfer functions relating these variables. Six of these transfer functions involve the state variables and the input variables while the remaining six involve the output variables with the input variables and the state variables.

Equation (25) in Section 4.1 describes the state vector $\underline{x}_S[(k+1)T_S]$ at the end of the switching cycle as a function of the state vector $\underline{x}_S(kT_S)$ at the beginning of the switching cycle, the duty ratio α_D , and the input vector \underline{u}_I . Rewriting (25) in the form of a difference equation, we have

$$\begin{aligned} \underline{x}_S[(k+1)T_S] - \underline{x}_S(kT_S) = & \left[\underline{A}_{ON}t_{ON} + \underline{A}_{OFF1}t_{OFF1} + \frac{\underline{A}_{ON}^2 t_{ON}^2 + \underline{A}_{OFF1}^2 t_{OFF1}^2}{2} \right. \\ & \left. + \underline{A}_{OFF1}\underline{A}_{ON}t_{OFF1}t_{ON} \right] \underline{x}_S(kT_S) \\ & + \left[\underline{B}_{ON}t_{ON} + \underline{B}_{OFF1}t_{OFF1} + \frac{\underline{A}_{ON}\underline{B}_{ON}t_{ON}^2}{2} \right. \\ & \left. + \frac{\underline{A}_{OFF1}\underline{B}_{OFF1}t_{OFF1}^2}{2} + \underline{A}_{OFF1}\underline{B}_{ON}t_{OFF1}t_{ON} \right] \underline{u}_I \end{aligned}$$

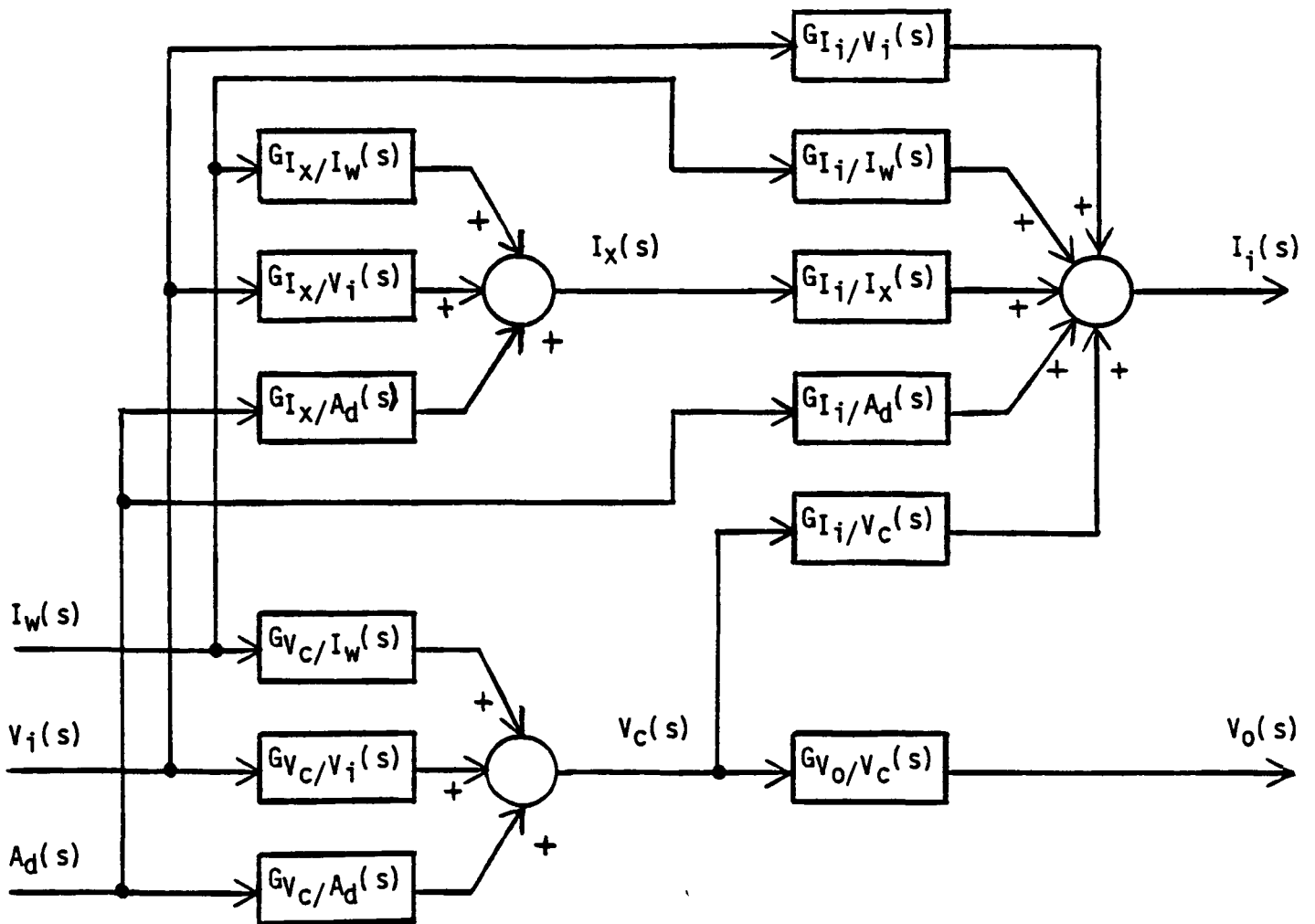


Fig. 11 Interconnection of functional blocks to characterize a converter power stage in the continuous-mmf mode.

The derivative $\frac{df}{dt}$ of any function $f(t)$ is defined as

$$\frac{df}{dt} = \lim_{\Delta t \rightarrow 0} \frac{f(t + \Delta t) - f(t)}{\Delta t}$$

Similarly, for changes that occur very slowly from one switching cycle to the next cycle, the derivative $\frac{d}{dt} \underline{x}_S$ can be approximated with $\{ \underline{x}_S[(k+1)T_S] - \underline{x}_S(kT_S) \} / T_S$ by letting $t = kT_S$ and $\Delta t = T_S$ because the period of the low-frequency perturbation signals is much larger than the switching period T_S . Therefore,

$$\begin{aligned} \frac{d}{dt} \underline{x}_{S,SS} &= \frac{\underline{x}_S[(k+1)T_S] - \underline{x}_S(kT_S)}{T_S} \\ &= \left[\underline{A}_{ON}\alpha_D + \underline{A}_{OFF}1(1-\alpha_D) + \frac{\underline{A}_{ON}^2\alpha_D^2T_S + \underline{A}_{OFF}^2(1-\alpha_D)^2T_S}{2} \right. \\ &\quad \left. + \underline{A}_{OFF}1\underline{A}_{ON}(1-\alpha_D)\alpha_DT_S \right] \underline{x}_{S,SS} \\ &\quad + \left[\underline{B}_{ON}\alpha_D + \underline{B}_{OFF}1(1-\alpha_D) + \frac{\underline{A}_{ON}\underline{B}_{ON}\alpha_D^2T_S + \underline{A}_{OFF}1\underline{B}_{OFF}1(1-\alpha_D)^2T_S}{2} \right. \\ &\quad \left. + \underline{A}_{OFF}1\underline{B}_{ON}(1-\alpha_D)\alpha_DT_S \right] \underline{u}_I \end{aligned} \quad (42)$$

Since (42) is derived from a difference equation involving the state vectors at the beginning of successive switching cycles, it is able to predict the stroboscopic variations of the state vector at the beginning of each switching cycle, while information about the state vector at time durations in between the beginning of successive switching cycles is lost. To separate the state vector observed at stroboscopic time intervals from the continuous state

vector $\underline{x}_s(t)$, the subscript ss has been used in (42) to denote the stroboscopic state vector which is valid only at the beginning of each switching cycle. Therefore, equation (42) is a matrix differential equation describing the stroboscopic variation of the state variables at the beginning of each switching cycle. It can be rewritten in the form

$$\frac{d}{dt} \begin{bmatrix} v_{C,ss} \\ i_{X,ss} \end{bmatrix} = \begin{bmatrix} f_V(v_{C,ss}, i_{X,ss}, \alpha_D, v_I, i_W) \\ f_I(v_{C,ss}, i_{X,ss}, \alpha_D, v_I, i_W) \end{bmatrix} \quad (43)$$

Equation (43) can be viewed as a differential equation with time-varying coefficients because the duty ratio α_D , which is time-varying from cycle to cycle under small-signal perturbation, appears as a coefficient associated with the state vector \underline{x}_s and the input vector \underline{u}_I . Although α_D does not appear explicitly as an input variable in the input vector \underline{u}_I in the equations derived in Sections 3 and 4, it is an important input variable controlling the energy flow in the power stage of a converter. Under small-signal perturbation around the equilibrium operating point, (43) can be rewritten as a system of two linear differential equations with constant coefficients involving the small-signal variables $\underline{x}_{s,ss} = [v_{C,ss} \ i_{X,ss}]^T$ and α_d, v_i , and i_w [4] :

$$\frac{d}{dt} \underline{x}_{s,ss} = \begin{bmatrix} \frac{\partial f_V}{\partial v_{C,ss}} & \frac{\partial f_V}{\partial i_{X,ss}} \\ \frac{\partial f_I}{\partial v_{C,ss}} & \frac{\partial f_I}{\partial i_{X,ss}} \end{bmatrix} \begin{bmatrix} v_{C,ss} \\ i_{X,ss} \end{bmatrix} + \begin{bmatrix} \frac{\partial f_V}{\partial \alpha_D} & \frac{\partial f_V}{\partial v_I} & \frac{\partial f_V}{\partial i_W} \\ \frac{\partial f_I}{\partial \alpha_D} & \frac{\partial f_I}{\partial v_I} & \frac{\partial f_I}{\partial i_W} \end{bmatrix} \begin{bmatrix} \alpha_d \\ v_i \\ i_w \end{bmatrix} \quad (44)$$

where the partial derivatives in (44) are evaluated at the equilibrium operating point. After the partial derivatives have been evaluated, (44) is seen to be a system of linear differential equations with constant coefficients as shown in (45).

$$\frac{d}{dt} \begin{bmatrix} v_{C,ss} \\ i_{X,ss} \end{bmatrix} = \begin{bmatrix} a_{11} & a_{12} \\ a_{21} & a_{22} \end{bmatrix} \begin{bmatrix} v_{C,ss} \\ i_{X,ss} \end{bmatrix} + \begin{bmatrix} b_{11} & b_{12} & b_{13} \\ b_{21} & b_{22} & b_{23} \end{bmatrix} \begin{bmatrix} \alpha_d \\ v_j \\ i_w \end{bmatrix} \quad (45)$$

where

$$a_{11} = \left. \frac{\partial f_V}{\partial v_{C,SS}} \right|_* \quad (46 a)$$

$$a_{12} = \left. \frac{\partial f_V}{\partial i_{X,SS}} \right|_* \quad (46 b)$$

$$b_{11} = \left. \frac{\partial f_V}{\partial \alpha_D} \right|_* \quad (46 c)$$

$$b_{12} = \left. \frac{\partial f_V}{\partial v_I} \right|_* \quad (46 d)$$

$$b_{13} = \left. \frac{\partial f_V}{\partial i_W} \right|_* \quad (46 e)$$

$$a_{21} = \left. \frac{\partial f_I}{\partial v_{C,SS}} \right|_* \quad (46 f)$$

$$a_{22} = \left. \frac{\partial f_I}{\partial i_{X,SS}} \right|_* \quad (46 g)$$

$$b_{21} = \left. \frac{\partial f_I}{\partial \alpha_D} \right|_* \quad (46 h)$$

$$b_{22} = \left. \frac{\partial f_I}{\partial v_I} \right|_* \quad (46 i)$$

$$b_{23} = \left. \frac{\partial f_I}{\partial i_W} \right|_* \quad (46 j)$$

The * symbols in Eqs. (46) indicate evaluation of the partial derivatives at the equilibrium operating point $[V_C(kT_S) \ I_X(kT_S)]^T$. Applying the Laplace transformation to (45), which represents a system of two small-signal linear differential equations with constant coefficients, gives

$$\begin{bmatrix} s - a_{11} & -a_{12} \\ -a_{21} & s - a_{22} \end{bmatrix} \begin{bmatrix} V_C(s) \\ I_X(s) \end{bmatrix} = \begin{bmatrix} b_{11} & b_{12} & b_{13} \\ b_{21} & b_{22} & b_{23} \end{bmatrix} \begin{bmatrix} A_d(s) \\ V_i(s) \\ I_w(s) \end{bmatrix}$$

Thus,

$$\begin{bmatrix} V_C(s) \\ I_X(s) \end{bmatrix} = \frac{\begin{bmatrix} s - a_{22} & a_{12} \\ a_{21} & s - a_{11} \end{bmatrix} \begin{bmatrix} b_{11} & b_{12} & b_{13} \\ b_{21} & b_{22} & b_{23} \end{bmatrix} \begin{bmatrix} A_d(s) \\ V_i(s) \\ I_w(s) \end{bmatrix}}{(s - a_{11})(s - a_{22}) - a_{12} a_{21}} \quad (47)$$

For example, the transfer function between the Laplace transformed small-signal capacitor voltage $V_C(s)$ and the transformation of a small-signal disturbance of the duty ratio $A_d(s)$ is

$$G_{V_C/A_d}(s) = \frac{V_C(s)}{A_d(s)} = \frac{b_{11}(s - a_{22}) + a_{12} b_{21}}{s^2 - s(a_{11} + a_{22}) + a_{11} a_{22} - a_{12} a_{21}} \quad (48)$$

All six transfer functions relating the two state variables and the three input variables are of the form indicated in (48), with one zero and a pair of complex poles. Table 1 lists the constants for these transfer functions.

The transfer function relating the capacitor voltage and the load voltage is derived in a straightforward manner from Fig. 9(d). Starting in the time domain,

Table 1. Six Small-Signal Transfer Functions for the Two State Variables Under Continuous-Mmf-Mode Operation.

FUNCTION FORM			$\frac{G (1 + s/Z)}{1 + 2\zeta (s/\omega_0) + (s/\omega_0)^2}$
NATURAL RESONANT FREQUENCY			$\omega_0 = \sqrt{a_{11} a_{22} - a_{12} a_{21}}$
DAMPING RATIO			$\zeta = - (a_{11} + a_{22}) / 2\omega_0$
FUNCTION	GAIN CONSTANT G	ZERO Z	
$G_{V_C/A_d}(s)$	$\frac{a_{12} b_{21} - a_{22} b_{11}}{\omega_0^2}$	$\frac{a_{12} b_{21} - a_{22} b_{11}}{b_{11}}$	
$G_{V_C/V_i}(s)$	$\frac{a_{12} b_{22} - a_{22} b_{12}}{\omega_0^2}$	$\frac{a_{12} b_{22} - a_{22} b_{12}}{b_{12}}$	
$G_{V_C/I_w}(s)$	$\frac{a_{12} b_{23} - a_{22} b_{13}}{\omega_0^2}$	$\frac{a_{12} b_{23} - a_{22} b_{13}}{b_{13}}$	
$G_{I_X/A_d}(s)$	$\frac{a_{21} b_{11} - a_{11} b_{21}}{\omega_0^2}$	$\frac{a_{21} b_{11} - a_{11} b_{21}}{b_{21}}$	
$G_{I_X/V_i}(s)$	$\frac{a_{21} b_{12} - a_{11} b_{22}}{\omega_0^2}$	$\frac{a_{21} b_{12} - a_{11} b_{22}}{b_{22}}$	
$G_{I_X/I_w}(s)$	$\frac{a_{21} b_{13} - a_{11} b_{23}}{\omega_0^2}$	$\frac{a_{21} b_{13} - a_{11} b_{23}}{b_{23}}$	

$$v_0 = - \left(v_C + r_C C \frac{dv_C}{dt} \right)$$

Transforming to the s domain,

$$\begin{aligned} V_0(s) &= - \left(V_C(s) + s r_C C V_C(s) \right) \\ &= - \left(1 + s r_C C \right) V_C(s) \end{aligned} \quad (49)$$

So far, transfer functions have been derived for the stroboscopic variations of the state variables at the beginning of each switching cycle. However, the information obtained from these stroboscopic variations alone is not adequate to characterize the power stage in the small-signal frequency domain. In the discontinuous- mmf mode, the total instantaneous value of the reactor exciting current is always equal to zero at the beginning of each switching cycle. That is, $i_X(kT_S)$ is identically equal to zero, thus making $i_{X,ss}$ equal to zero since $i_{X,ss}$ is equal to the small-signal variational part of $i_X(kT_S)$. As a result, using $i_{X,ss}$ to derive the input impedance of a power stage of a dc-to-dc converter operating in the discontinuous- mmf mode indicates an infinite input impedance, which is erroneous. Because of the switching nature of the power stage and the low-pass characteristics of the output filter, it is the energy flow over one switching cycle, not the instantaneous power flow, that is regulated. Therefore, it is more appropriate to use the energy flow over one switching cycle to derive transfer functions for the two output variables — the supply current and the load voltage.

Going back to the large-signal instantaneous variables, the energy W_0 delivered to load resistance R_L in one switching cycle is

$$w_0 = \int_{kT_s}^{(k+1)T_s} \frac{(v_0(t))^2}{R_L} dt$$

The load voltage can be approximated as

$$v_0(t) = v_{0,k} + v_{OR}(t)$$

where $v_{0,k}$ is the average load voltage over the k th switching cycle and $v_{OR}(t)$ is the ripple voltage across the load, which has an average value equal to zero over one switching cycle. Therefore,

$$\begin{aligned} w_0 &= \int_{kT_s}^{(k+1)T_s} \frac{(v_{0,k} + v_{OR}(t))^2}{R_L} dt \\ &= \int_{kT_s}^{(k+1)T_s} \frac{(v_{0,k})^2}{R_L} dt + \int_{kT_s}^{(k+1)T_s} \frac{(v_{OR}(t))^2}{R_L} dt \end{aligned}$$

Because of the stringent restriction placed on the ripple voltage across the load of a dc-to-dc converter, the capacitor is usually chosen with sufficient capacitance and low enough ESR to reduce the ripple voltage across the load to a level which is very small compared to the nominal load voltage. Therefore, $v_{OR}(t)$ is very small compared to $v_{0,k}$, and

$$\begin{aligned} w_0 &\approx \int_{kT_s}^{(k+1)T_s} \frac{(v_{0,k})^2}{R_L} dt \\ &= \frac{(v_{0,k})^2 T_s}{R_L} \end{aligned}$$

Since the ripple voltage $v_{OR}(t)$ is negligible when compared to the average load voltage $v_{0,k}$, the load voltage at the beginning of each switching cycle $v_0(kT_s)$ is very close to the average load voltage $v_{0,k}$. Hence,

$$w_0 = \frac{(v_{0,k})^2 T_s}{R_L} \approx \frac{(v_0(kT_s))^2 T_s}{R_L}$$

Therefore, using the stroboscopic load voltage $v_0(kT_S)$ to account for the energy delivered to the load over one switching cycle is a good approximation. As a result, the transfer function derived in (49), which is valid for the stroboscopic load voltage $v_{0,ss}$, is also quite accurate in describing the small-signal value of the average load voltage $v_{0,k}$ over one switching cycle.

Unlike the load voltage, the supply current usually has a relatively high amount of ripple content compared to its average value. The energy drawn from the power supply over one switching cycle is

$$W_I = \int_{kT_S}^{(k+1)T_S} v_I i_I dt$$

Using $v_{I,k}$ and $i_{I,k}$ to represent the average supply voltage and average supply current over one switching cycle, and $v_{IR}(t)$ and $i_{IR}(t)$ to represent the ripples in the supply voltage and supply current,

$$\begin{aligned} W_I &= \int_{kT_S}^{(k+1)T_S} (v_{I,k} + v_{IR}(t)) (i_{I,k} + i_{IR}(t)) dt \\ &= T_S v_{I,k} i_{I,k} + \int_{kT_S}^{(k+1)T_S} v_{IR}(t) i_{IR}(t) dt \end{aligned}$$

The ripple $v_{IR}(t)$ in the supply voltage is usually negligible compared to $v_{I,k}$, the supply voltage averaged over one switching cycle. Although the ripple $i_{IR}(t)$ in the supply current is not negligible compared to $i_{I,k}$, the supply current averaged over one switching cycle, it is finite in magnitude. Therefore, the contribution to W_I is mainly from the first integral, i.e.

$$W_I \approx T_S v_{I,k} i_{I,k}$$

Since $i_{I,k}$ is the supply current averaged over one switching cycle, by definition

$$i_{I,k} = \frac{1}{T_S} \int_{kT_S}^{(k+1)T_S} i_X(t) dt$$

Since the ripple $v_{IR}(t)$ in the supply voltage over one switching cycle is small, the value of $v_{I,k}$ is very close to the actual instantaneous voltage $v_I(t)$. Therefore, the power drawn from the power supply on a per cycle basis is

$$\begin{aligned} P_I &= W_I / T_S \\ &\approx v_{I,k} i_{I,k} \\ &\approx v_I i_{I,k} \end{aligned}$$

Hence, the modeling of the input port of a power stage should be derived from the supply current $i_{I,k}$ averaged over one switching cycle. To characterize the small-signal average supply current $i_{I,k}$, it is convenient to start by going back to the large-signal instantaneous description of the state variables. Two matrices \underline{M}_{ON} and \underline{M}_{OFF1} are introduced such that when the transistor is conducting,

$$i_I(t) = \underline{M}_{ON} \underline{x}_S(t) = \underline{M}_{ON} \begin{bmatrix} v_C(t) \\ i_X(t) \end{bmatrix}$$

and when the diode is conducting,

$$i_I(t) = \underline{M}_{OFF1} \underline{x}_S(t) = \underline{M}_{OFF1} \begin{bmatrix} v_C(t) \\ i_X(t) \end{bmatrix}$$

For both SCVU and TCVU, the supply current is equal to the reflected reactor exciting current when the transistor is conducting, and is zero otherwise. Therefore

$$\underline{M}_{ON} = [0 \ \gamma] \quad (50, CVU)$$

$$\underline{M}_{OFF1} = [0 \ 0] \quad (51, CVU)$$

Using these definitions, the average supply current in the k th switching cycle $i_{I,k}$ is defined as

$$i_{I,k} = \frac{1}{T_S} \int_{kT_S}^{kT_S + \alpha_D T_S} \underline{M}_{ON} \underline{x}_S(t) dt + \frac{1}{T_S} \int_{kT_S + \alpha_D T_S}^{(k+1)T_S} \underline{M}_{OFF1} \underline{x}_S(t) dt \quad (52)$$

For α_D , v_I , and i_W constant throughout the k th switching cycle, substituting the expressions for $\underline{x}_S(t)$ from (14) and (16) into (52) gives

$$\begin{aligned} i_{I,k} &= \frac{\underline{M}_{ON}}{T_S} \int_{kT_S}^{kT_S + \alpha_D T_S} \left[e^{\underline{A}_{ON}(t - kT_S)} \underline{x}_S(kT_S) + \underline{A}_{ON}^{-1} (e^{\underline{A}_{ON}(t - kT_S)} - \underline{I}) \underline{B}_{ON} \underline{u}_I \right] dt \\ &+ \frac{\underline{M}_{OFF1}}{T_S} \int_{kT_S + \alpha_D T_S}^{(k+1)T_S} \left[e^{\underline{A}_{OFF1}(t - kT_S - t_{ON})} \underline{x}_S(kT_S + t_{ON}) \right. \\ &\quad \left. + \underline{A}_{OFF1}^{-1} (e^{\underline{A}_{OFF1}(t - kT_S - t_{ON})} - \underline{I}) \underline{B}_{OFF1} \underline{u}_I \right] dt \\ &= \frac{\underline{M}_{ON}}{T_S} \left[\underline{A}_{ON}^{-1} e^{\underline{A}_{ON}(t - kT_S)} \underline{x}_S(kT_S) + \underline{A}_{ON}^{-1} (\underline{A}_{ON}^{-1} e^{\underline{A}_{ON}(t - kT_S)} - \underline{I} t) \underline{B}_{ON} \underline{u}_I \right]_{kT_S}^{kT_S + \alpha_D T_S} \\ &+ \frac{\underline{M}_{OFF1}}{T_S} \left[\underline{A}_{OFF1}^{-1} e^{\underline{A}_{OFF1}(t - kT_S - t_{ON})} \underline{x}_S(kT_S + t_{ON}) \right. \\ &\quad \left. + \underline{A}_{OFF1}^{-1} (\underline{A}_{OFF1}^{-1} e^{\underline{A}_{OFF1}(t - kT_S - t_{ON})} - \underline{I} t) \underline{B}_{OFF1} \underline{u}_I \right]_{kT_S + \alpha_D T_S}^{(k+1)T_S} \end{aligned}$$

$$\begin{aligned}
i_{I,k} = & \frac{M_{ON}}{T_S} \left[\underline{A}_{ON}^{-1} \left(e^{\underline{A}_{ON}\alpha_D T_S} \underline{-I} \right) \underline{x}_S(kT_S) + \underline{A}_{ON}^{-1} \left(\underline{A}_{ON}^{-1} \left(e^{\underline{A}_{ON}\alpha_D T_S} \underline{-I} \right) - \underline{I} \alpha_D T_S \right) \underline{B}_{ON} \underline{u}_I \right] \\
& + \frac{M_{OFF1}}{T_S} \left[\underline{A}_{OFF1}^{-1} \left[e^{\underline{A}_{OFF1}(1-\alpha_D) T_S} \underline{-I} \right] \underline{x}_S(kT_S + t_{ON}) \right. \\
& \quad \left. + \underline{A}_{OFF1}^{-1} \left(\underline{A}_{OFF1}^{-1} \left(e^{\underline{A}_{OFF1}(1-\alpha_D) T_S} \underline{-I} \right) - \underline{I} (1-\alpha_D) T_S \right) \underline{B}_{OFF1} \underline{u}_I \right]
\end{aligned}$$

Since \underline{M}_{OFF1} is equal to $[0 \ 0]$ for both SCVU and TCVU, it is not necessary to carry any terms premultiplied by \underline{M}_{OFF1} in the above equations as there is no contribution to $i_{I,k}$ from these terms. The above equations, however, are derived for all four basic converters. In the case of the voltage step-up converter, deletion of \underline{M}_{OFF1} and its associated terms is not possible as \underline{M}_{OFF1} is equal to $[0 \ 1]$. As a result, \underline{M}_{OFF1} and its associated terms are not removed from the above equations so that the reader can trace the parallel paths of derivation of $i_{I,k}$ between the Phase A Report and this Phase B Report. Substituting $t = kT_S + t_{ON}$ into (14),

$$\underline{x}_S(kT_S + t_{ON}) = e^{\underline{A}_{ON}\alpha_D T_S} \underline{x}_S(kT_S) + \underline{A}_{ON}^{-1} \left(e^{\underline{A}_{ON}\alpha_D T_S} \underline{-I} \right) \underline{B}_{ON} \underline{u}_I$$

Therefore,

$$\begin{aligned}
i_{I,k} = & \frac{M_{ON}}{T_S} \left[\underline{A}_{ON}^{-1} \left(e^{\underline{A}_{ON}\alpha_D T_S} \underline{-I} \right) \underline{x}_S(kT_S) + \underline{A}_{ON}^{-1} \left(\underline{A}_{ON}^{-1} \left(e^{\underline{A}_{ON}\alpha_D T_S} \underline{-I} \right) - \underline{I} \alpha_D T_S \right) \underline{B}_{ON} \underline{u}_I \right] \\
& + \frac{M_{OFF1}}{T_S} \left[\underline{A}_{OFF1}^{-1} \left(e^{\underline{A}_{OFF1}(1-\alpha_D) T_S} \underline{-I} \right) \left(e^{\underline{A}_{ON}\alpha_D T_S} \underline{x}_S(kT_S) \right. \right. \\
& \quad \left. \left. + \underline{A}_{ON}^{-1} \left(e^{\underline{A}_{ON}\alpha_D T_S} \underline{-I} \right) \underline{B}_{ON} \underline{u}_I \right) \right. \\
& \quad \left. + \underline{A}_{OFF1}^{-1} \left(\underline{A}_{OFF1}^{-1} \left(e^{\underline{A}_{OFF1}(1-\alpha_D) T_S} \underline{-I} \right) - \underline{I} (1-\alpha_D) T_S \right) \underline{B}_{OFF1} \underline{u}_I \right]
\end{aligned} \tag{53}$$

Expanding the state transition matrices $e^{\frac{A_{ON}\alpha_D T_S}{2}}$ and $e^{\frac{A_{OFF}1(1-\alpha_D)T_S}{2}}$ and retaining only up to second-order terms in T_S ,

$$\begin{aligned}
 i_{I,k} = \underline{M}_{ON} \left[(\alpha_D \underline{I} + \frac{A_{ON}\alpha_D^2 T_S}{2}) \underline{x}_{S,SS} + \frac{B_{ON}\alpha_D^2 T_S}{2} \underline{u}_I \right] \\
 + \underline{M}_{OFF} \left[((1-\alpha_D) \underline{I} + \frac{A_{OFF}1(1-\alpha_D)^2 T_S}{2} + A_{ON}(1-\alpha_D)\alpha_D T_S) \underline{x}_{S,SS} \right. \\
 \left. + (\frac{B_{OFF}1(1-\alpha_D)^2 T_S}{2} + B_{ON}(1-\alpha_D)\alpha_D T_S) \underline{u}_I \right] \quad (54)
 \end{aligned}$$

where $\underline{x}_S(kT_S)$ has been replaced by $\underline{x}_{S,SS}$ to follow the notation used earlier. Equation (54) can be rewritten as

$$i_I = f(\underline{x}_{S,SS}, \alpha_D, v_I, i_W) \quad (55)$$

Linearizing (54) and applying the Laplace transformation,

$$I_i(s) = p_{11} V_c(s) + p_{12} I_x(s) + q_{11} A_d(s) + q_{12} V_i(s) + q_{13} I_w(s) \quad (56)$$

where

$$\begin{aligned}
 p_{11} = \left. \frac{\partial f}{\partial v_{C,SS}} \right|_* = \underline{M}_{ON} \left(A_D \underline{I} + \frac{A_{ON}A_D^2 T_S}{2} \right) [1 \ 0]^T \\
 + \underline{M}_{OFF} \left((1-A_D) \underline{I} + \frac{A_{OFF}1(1-A_D)^2 T_S}{2} + A_{ON}(1-A_D)A_D T_S \right) [1 \ 0]^T \quad (57a)
 \end{aligned}$$

$$\begin{aligned}
 p_{12} = \left. \frac{\partial f}{\partial i_{X,SS}} \right|_* = \underline{M}_{ON} \left(A_D \underline{I} + \frac{A_{ON}A_D^2 T_S}{2} \right) [0 \ 1]^T \\
 + \underline{M}_{OFF} \left((1-A_D) \underline{I} + \frac{A_{OFF}1(1-A_D)^2 T_S}{2} + A_{ON}(1-A_D)A_D T_S \right) [0 \ 1]^T \quad (57b)
 \end{aligned}$$

$$\begin{aligned}
 q_{11} = \left. \frac{\partial f}{\partial \alpha_D} \right|_* &= \underline{M}_{ON} \left[\left(\underline{I} + \underline{A}_{ON} \underline{A}_D T_S \right) \underline{X}_S(kT_S) + \underline{B}_{ON} \underline{A}_D T_S \underline{U}_I \right] \\
 &+ \underline{M}_{OFF1} \left[\left(-\underline{I} - \underline{A}_{OFF1}(1-\underline{A}_D) T_S + \underline{A}_{ON}(1-2\underline{A}_D) T_S \right) \underline{X}_S(kT_S) \right. \\
 &\quad \left. + \left(-\underline{B}_{OFF1}(1-\underline{A}_D) T_S + \underline{B}_{ON}(1-2\underline{A}_D) T_S \right) \underline{U}_I \right]
 \end{aligned} \tag{57 c}$$

$$\begin{aligned}
 q_{12} = \left. \frac{\partial f}{\partial v_I} \right|_* &= \left[\frac{\underline{M}_{ON} \underline{B}_{ON} \underline{A}_D^2 T_S}{2} + \frac{\underline{M}_{OFF1} \underline{B}_{OFF1} (1-\underline{A}_D)^2 T_S}{2} \right. \\
 &\quad \left. + \underline{M}_{OFF1} \underline{B}_{ON} (1-\underline{A}_D) \underline{A}_D T_S \right] [1 \ 0 \ 0 \ 0]^T
 \end{aligned} \tag{57 d}$$

$$\begin{aligned}
 q_{13} = \left. \frac{\partial f}{\partial i_W} \right|_* &= \left[\frac{\underline{M}_{ON} \underline{B}_{ON} \underline{A}_D^2 T_S}{2} + \frac{\underline{M}_{OFF1} \underline{B}_{OFF1} (1-\underline{A}_D)^2 T_S}{2} \right. \\
 &\quad \left. + \underline{M}_{OFF1} \underline{B}_{ON} (1-\underline{A}_D) \underline{A}_D T_S \right] [0 \ 1 \ 0 \ 0]^T
 \end{aligned} \tag{57 e}$$

This analysis demonstrates that the small-signal average supply current $I_i(s)$ depends on the small-signal variables $V_C(s)$, $I_X(s)$, $A_D(s)$, $V_i(s)$, and $I_W(s)$. From Section 5.1, the capacitor voltage v_C and the inductor current i_X were found to depend on the duty ratio α_d , the supply voltage v_i , and the load-disturbance current i_W . Now perturb the power stage with a small-signal applied to the supply voltage, holding the duty ratio and the load-disturbance current constant. If the perturbation is performed at a frequency close to half of the switching frequency, then $V_C(s)$ and $I_X(s)$ will be well attenuated by the pair of complex poles listed in Table 1. As a result, according to (56),

$$I_i(s) \approx q_{12} V_i(s)$$

or

$$\frac{V_i(s)}{I_i(s)} = \frac{1}{q_{12}}$$

This implies that the input impedance of the power stage is resistive at very high frequencies because the $G_{I_i/V_i}(s)$ derived from (57c) is just a numerical constant independent of frequency. This contradicts the observed phenomenon that a power stage possesses an inductive input impedance when the perturbation frequency is relatively high. Tracing the path of the modeling process, this discrepancy can be attributed to the assumption that \underline{u}_I is piecewise-constant over one switching period.

Although it has been deduced that (56), with the constants calculated from (57a) to (57e), is not accurate enough at high frequencies, a dc analysis shows that the numerical constants from (57a) through (57e) are the correct gain constants for the various transfer functions from the state variables and input variables to the average supply current.

Now examine the dependence of the supply current i_i on the three input variables, duty ratio α_d , input voltage v_i , and load-disturbance current i_w . Although the duty ratio α_d has been treated as a continuous variable for small-signal perturbation at frequencies below half of the switching frequency, it is actually a discrete time variable. In each switching period, there is only one single value for the duty ratio α_d , and hence also a single value for α_d . As a result, the dependence of the average supply current i_i on the duty ratio α_d , taking both variables in the same switching period, is frequency independent. Therefore, the transfer function from the duty ratio to the supply current is just a proportionality constant as defined in (57c).

To exactly model how i_i will vary under a small-signal perturbation at the supply voltage requires the modeling of \underline{u}_I as a time-varying source over one switching cycle, which then complicates the modeling excessively. Since the supply current is identical to the inductor current times the turn ratio during part of the switching cycle, the frequency dependence of the average supply current on the supply voltage will be similar to the frequency dependence of the inductor current on the supply voltage. As a result, the frequency dependence of $I_i(s)$ on $V_i(s)$ will be well approximated if it is assumed that the poles and zeros of $G_{I_i/V_i}(s)$ are equal to the poles and zeros of $G_{I_X/V_i}(s)$. As crude an assumption as this may seem to be, it provides an adequate approximation of $G_{I_i/V_i}(s)$ when compared to experimentally measured data. Such an assumption may be justified by the following explanation. Had $G_{I_i/V_i}(s)$ been approximated with the numerical constant q_{12} given in (57d), the input impedance function obtained from such an analysis would still be quite accurate at dc and very low frequencies. Therefore, using q_{12} given in (57d) as the dc gain of $G_{I_i/V_i}(s)$ and the poles and zeros of $G_{I_X/V_i}(s)$ as the poles and zeros of $G_{I_i/V_i}(s)$ gives a fair approximation of $G_{I_i/V_i}(s)$ from dc up to half of the switching frequency. Similarly, the transfer function $G_{I_i/I_W}(s)$ is approximated by taking the numerical constant q_{13} from (57e) as its dc gain constant and the poles and zeros of $G_{I_X/I_W}(s)$ as its poles and zeros. The six transfer functions describing the load voltage and the supply current are listed in Table 2.

Substituting the matrices \underline{A}_{ON} , \underline{A}_{OFF1} , \underline{B}_{ON} , and \underline{B}_{OFF1} from (19,CVU) to (22,CVU) into (42), and comparing with (43),

Table 2. Six Transfer Functions Describing the Load Voltage and the Supply Current for Continuous-Mmf-Mode Operation.

FUNCTION FORM		$\frac{G (1 + s/Z)}{1 + 2\zeta (s/\omega_0) + (s/\omega_0)^2}$	
NATURAL RESONANT FREQUENCY		$\omega_0 = \sqrt{a_{11} a_{22} - a_{12} a_{21}}$	
DAMPING RATIO		$\zeta = - (a_{11} + a_{22}) / 2\omega_0$	
FUNCTION	GAIN CONSTANT	G	ZERO Z
$G_{I_i/V_i}(s)$	q_{12}		$\frac{a_{21} b_{12} - a_{11} b_{22}}{b_{22}}$
$G_{I_i/I_w}(s)$	q_{13}		$\frac{a_{21} b_{13} - a_{11} b_{23}}{b_{23}}$
FUNCTION			
$G_{V_o/V_c}(s) = - (1 + s r_c C)$		$G_{I_i/I_x}(s) = p_{12}$	
$G_{I_i/V_c}(s) = p_{11}$		$G_{I_i/A_d}(s) = q_{11}$	

$$\begin{aligned}
f_V = & -\omega_a v_{C,SS} \left(1 - \frac{\omega_a T_S}{2} + \frac{\rho R_L (1-\alpha_D)^2 T_S}{2L_S} \right) + \frac{\gamma R_L \omega_a (v_I - v_Q) (1-\alpha_D) \alpha_D T_S}{L_S} \\
& + R_L \omega_a i_{X,SS} \left((1-\alpha_D) - \omega_g (1-\alpha_D) \alpha_D T_S - \frac{(\omega_a + \omega_h) (1-\alpha_D)^2 T_S}{2} \right) \\
& - R_L \omega_a i_W \left(1 - \frac{\omega_a T_S}{2} - \frac{\omega_e (1-\alpha_D)^2 T_S}{2} \right) - \frac{R_L \omega_a v_D (1-\alpha_D)^2 T_S}{2L_S}
\end{aligned}$$

and

$$\begin{aligned}
f_I = & -\frac{\rho v_{C,SS}}{L_S} \left((1-\alpha_D) - \frac{\omega_a (1-\alpha_D)^2 T_S}{2} - \frac{\omega_h (1-\alpha_D)^2 T_S}{2} \right) \\
& - i_{X,SS} \left(\omega_g \alpha_D + \omega_h (1-\alpha_D) - \frac{(\omega_g \alpha_D + \omega_h (1-\alpha_D))^2 T_S}{2} + \frac{\rho R_L \omega_a (1-\alpha_D)^2 T_S}{2L_S} \right) \\
& + \frac{\gamma (v_I - v_Q)}{L_S} \left(\alpha_D - \omega_h (1-\alpha_D) \alpha_D T_S - \frac{\omega_g \alpha_D^2 T_S}{2} \right) \\
& + i_W \left(\omega_e (1-\alpha_D) + \frac{\rho R_L \omega_a (1-\alpha_D)^2 T_S}{2L_S} - \frac{\omega_e \omega_h (1-\alpha_D)^2 T_S}{2} \right) \\
& - \frac{v_D}{L_S} \left((1-\alpha_D) - \frac{\omega_h (1-\alpha_D)^2 T_S}{2} \right)
\end{aligned}$$

Computing the derivatives according to (46a) through (46j) gives

$$a_{11} = -\omega_a \left(1 - \frac{\omega_a T_S}{2} + \frac{\rho R_L (1-\alpha_D)^2 T_S}{2L_S} \right) \quad (46a, CVU)$$

$$a_{12} = R_L \omega_a \left((1-\alpha_D) - \omega_g (1-\alpha_D) \alpha_D T_S - \frac{(\omega_a + \omega_h) (1-\alpha_D)^2 T_S}{2} \right) \quad (46b, CVU)$$

$$\begin{aligned}
 b_{11} = & \frac{R_L \omega_a V_0 (1-A_D) T_S}{L_S} - R_L \omega_a I_X (k T_S) (1 + \omega_g (1-2A_D) T_S - (\omega_a + \omega_h) (1-A_D) T_S) \\
 & - R_L \omega_a I_W \omega_e (1-A_D) T_S + \frac{\gamma R_L \omega_a (V_I - V_Q) (1-2A_D) T_S}{L_S} + \frac{R_L \omega_a V_D (1-A_D) T_S}{L_S}
 \end{aligned} \quad (46c, CVU)$$

$$b_{12} = \frac{\gamma R_L \omega_a (1-A_D) A_D T_S}{L_S} \quad (46d, CVU)$$

$$b_{13} = -R_L \omega_a \left(1 - \frac{\omega_a T_S}{2} - \frac{\omega_e (1-A_D)^2 T_S}{2} \right) \quad (46e, CVU)$$

$$a_{21} = -\frac{\rho}{L_S} \left((1-A_D) - \frac{\omega_a (1-A_D)^2 T_S}{2} - \frac{\omega_h (1-A_D)^2 T_S}{2} \right) \quad (46f, CVU)$$

$$a_{22} = - \left(\omega_g A_D + \omega_h (1-A_D) - \frac{(\omega_g A_D + \omega_h (1-A_D))^2 T_S}{2} + \frac{\rho R_L \omega_a (1-A_D)^2 T_S}{2 L_S} \right) \quad (46g, CVU)$$

$$\begin{aligned}
 b_{21} = & \frac{\rho V_0}{L_S} (1 - \omega_a A_D T_S - \omega_h (1-A_D) T_S) \\
 & - I_X (k T_S) (\omega_g - \omega_h - (\omega_g - \omega_h) (\omega_g A_D + \omega_h (1-A_D)) T_S - \frac{\rho R_L \omega_a (1-A_D) T_S}{L_S}) \\
 & - I_W \left(\omega_e + \frac{\rho R_L \omega_a A_D T_S}{L_S} - \omega_e \omega_h (1-A_D) T_S \right) + \frac{V_D}{L_S} (1 - \omega_h (1-A_D) T_S) \\
 & + \frac{\gamma (V_I - V_Q)}{L_S} (1 - \omega_h (1-2A_D) T_S - \omega_g A_D T_S)
 \end{aligned} \quad (46h, CVU)$$

$$b_{22} = \frac{\gamma}{L_S} \left(A_D - \frac{\omega_g A_D^2 T_S}{2} - \omega_h (1-A_D) A_D T_S \right) \quad (46i, CVU)$$

$$b_{23} = \left(\omega_e(1-A_D) + \frac{\rho R_L \omega_a(1-A_D^2)T_S}{2L_S} - \frac{\omega_e \omega_h(1-A_D)^2 T_S}{2} \right) \quad (46j, CVU)$$

After substituting the matrices \underline{A}_{ON} , \underline{A}_{OFF1} , \underline{B}_{ON} , and \underline{B}_{OFF1} from (19,CVU) to (22,CVU) and the matrices \underline{M}_{ON} and \underline{M}_{OFF1} from (50,CVU) and (51,CVU) into (57a) to (57e),

$$p_{11} = 0 \quad (57a, CVU)$$

$$p_{12} = \gamma A_D \left(1 - \frac{\omega_g A_D T_S}{2} \right) \quad (57b, CVU)$$

$$q_{11} = \gamma I_X(kT_S)(1-A_D \omega_g T_S) + \frac{\gamma^2(V_I - V_Q) A_D T_S}{L_S} \quad (57c, CVU)$$

$$q_{12} = \frac{\gamma^2 A_D^2 T_S}{2L_S} \quad (57d, CVU)$$

$$q_{13} = 0 \quad (57e, CVU)$$

5.2 Small-Signal Transfer Functions in the Discontinuous-Mmf Mode

In the discontinuous-mmf mode, the inductor current at the beginning of each switching cycle, $i_X(kT_S)$, is always equal to zero. As a result, $i_X(kT_S)$ is no longer a dynamic variable. As far as signal flow is concerned, the power stage can be modeled by the block diagram shown in Fig. 12.

Following the approximation of the derivatives shown in Section 5.1, and using (33) derived in Section 4.2,

$$\begin{aligned}
\frac{d}{dt} \underline{x}_{S,SS} = & \frac{1}{T_S} \left\{ \underline{A}_{ON} t_{ON} + \underline{A}_{OFF1} t_{OFF1} + \underline{A}_{OFF2} (T_S - t_{ON} - t_{OFF1}) \right. \\
& + \frac{\underline{A}_{ON}^2 t_{ON}^2 + \underline{A}_{OFF1}^2 t_{OFF1}^2 + \underline{A}_{OFF2}^2 (T_S - t_{ON} - t_{OFF1})^2}{2} \\
& + \underline{A}_{OFF1} \underline{A}_{ON} t_{OFF1} t_{ON} + \underline{A}_{OFF2} \underline{A}_{ON} (T_S - t_{ON} - t_{OFF1}) t_{ON} \\
& \left. + \underline{A}_{OFF2} \underline{A}_{OFF1} (T_S - t_{ON} - t_{OFF1}) t_{OFF1} \right\} \underline{x}_{S,SS} \\
& + \frac{1}{T_S} \left\{ \underline{B}_{ON} t_{ON} + \underline{B}_{OFF1} t_{OFF1} + \underline{B}_{OFF2} (T_S - t_{ON} - t_{OFF1}) \right. \\
& + \frac{\underline{A}_{ON} \underline{B}_{ON} t_{ON}^2 + \underline{A}_{OFF1} \underline{B}_{OFF1} t_{OFF1}^2 + \underline{A}_{OFF2} \underline{B}_{OFF2} (T_S - t_{ON} - t_{OFF1})^2}{2} \\
& + \underline{A}_{OFF1} \underline{B}_{ON} t_{OFF1} t_{ON} + \underline{A}_{OFF2} \underline{B}_{ON} (T_S - t_{ON} - t_{OFF1}) t_{ON} \\
& \left. + \underline{A}_{OFF2} \underline{B}_{OFF1} (T_S - t_{ON} - t_{OFF1}) t_{OFF1} \right\} \underline{u}_I
\end{aligned} \tag{58}$$

Rewriting (58),

$$\frac{d}{dt} \begin{bmatrix} v_{C,SS} \\ i_{X,SS} \end{bmatrix} = \begin{bmatrix} f_V(v_{C,SS}, \alpha_D, v_I, i_W) \\ 0 \end{bmatrix} \tag{59}$$

The derivative for $i_{X,SS}$ is zero because $i_X(kT_S)$, the inductor current at the beginning of a switching cycle, is identically equal to zero for every switching cycle. Linearizing (59) at the equilibrium operating point, a small-signal differential equation is obtained.

$$\frac{d}{dt} v_{C,SS} = \frac{\partial f_V}{\partial v_C} v_{C,SS} + \frac{\partial f_V}{\partial \alpha_D} \alpha_D + \frac{\partial f_V}{\partial v_I} v_I + \frac{\partial f_V}{\partial i_W} i_W \tag{60}$$

where the partial derivatives in (60) are evaluated at the equilibrium operating point. Rewriting (60),

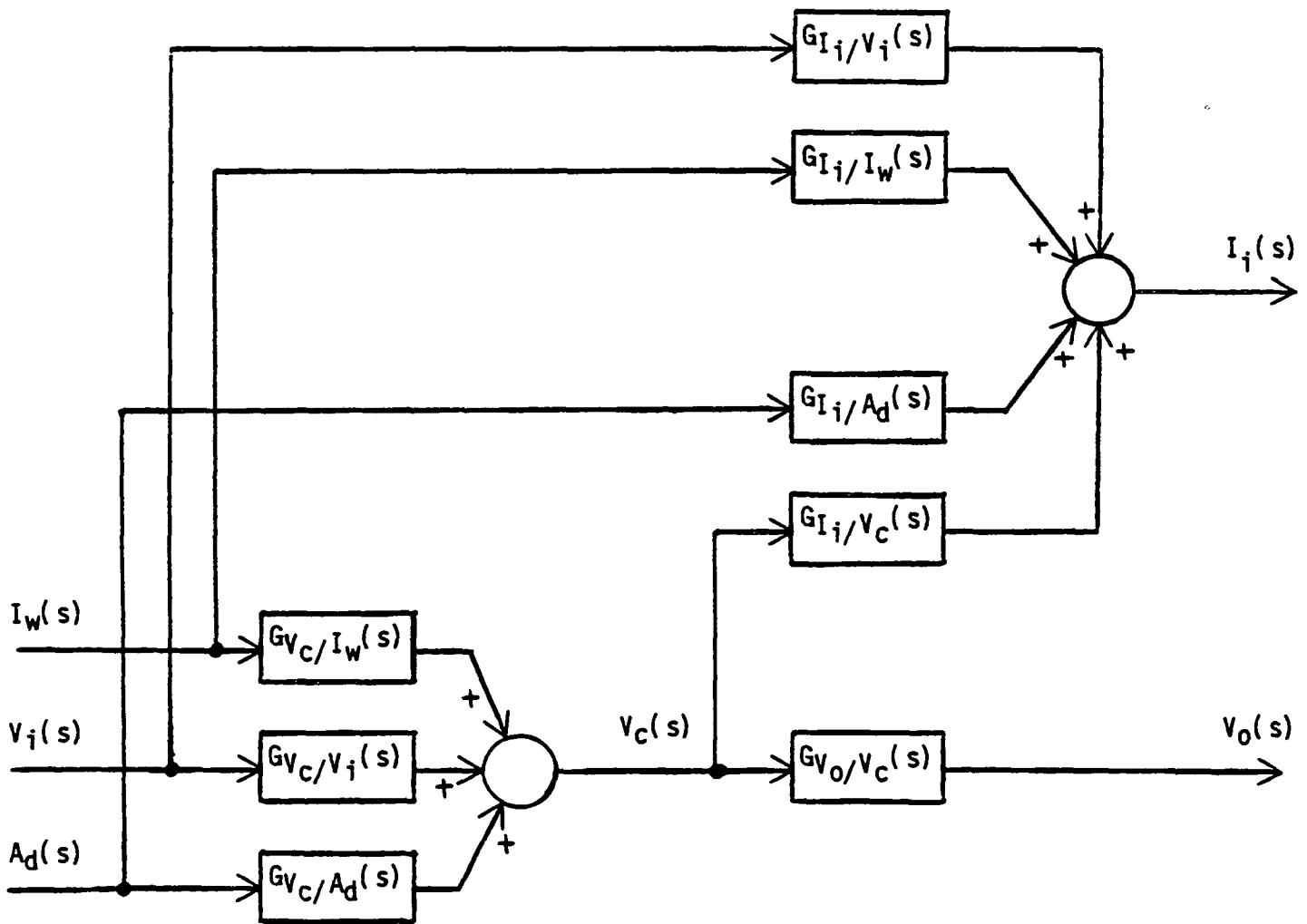


Fig. 12 Interconnection of functional blocks to characterize a converter power stage in the discontinuous-mmf mode.

$$\frac{d}{dt} v_{C,ss} = a_{11} v_{C,ss} + b_{11} \alpha_d + b_{12} v_i + b_{13} i_w \quad (61)$$

where

$$a_{11} = \left. \frac{\partial f_V}{\partial v_{C,SS}} \right|_* \quad (62a)$$

$$b_{11} = \left. \frac{\partial f_V}{\partial \alpha_D} \right|_* \quad (62b)$$

$$b_{12} = \left. \frac{\partial f_V}{\partial v_I} \right|_* \quad (62c)$$

$$b_{13} = \left. \frac{\partial f_V}{\partial i_W} \right|_* \quad (62d)$$

and the *'s in Eqs. (62) indicate that the partial derivatives are evaluated at the equilibrium operating point. Applying the Laplace transformation on (61) gives

$$s V_C(s) = a_{11} V_C(s) + b_{11} A_d(s) + b_{12} V_i(s) + b_{13} I_w(s)$$

Thus

$$V_C(s) = \frac{b_{11} A_d(s) + b_{12} V_i(s) + b_{13} I_w(s)}{(s - a_{11})} \quad (63)$$

and the three transfer functions relating $V_C(s)$ and the inputs are listed in Table 3.

As in the case of the continuous-mmf mode operation, the transfer function relating the load voltage and capacitor voltage is

$$G_{V_O/V_C}(s) = - (1 + s r_C C) \quad (64)$$

Table 3. Three Transfer Functions for the Ideal Capacitor Voltage Under Discontinuous-Mmf-Mode Operation

$G_{V_C/A_d}(s) = \frac{b_{11}}{s - a_{11}}$
$G_{V_C/V_i}(s) = \frac{b_{12}}{s - a_{11}}$
$G_{V_C/I_w}(s) = \frac{b_{13}}{s - a_{11}}$

Similar to the modeling of the supply current in the continuous-mmf mode, the average supply current will be derived over one switching period as a function of other circuit variables :

$$i_{I,k} = \frac{1}{T_S} \int_{kT_S}^{kT_S + \alpha_D T_S} \underline{M}_{ON} \underline{x}_S(t) dt + \frac{1}{T_S} \int_{kT_S + \alpha_D T_S}^{kT_S + \alpha_D T_S + t_{OFF1}} \underline{M}_{OFF1} \underline{x}_S(t) dt \quad (65)$$

Since the inductor current is equal to zero in the time interval between $kT_S + \alpha_D T_S + t_{OFF1}$ and $(k+1)T_S$, the contribution to the average supply current during that time interval is also zero. Hence (65) does not contain the integral in the time interval from $kT_S + \alpha_D T_S + t_{OFF1}$ to $(k+1)T_S$. Similar to (54) in the continuous-mmf mode,

$$\begin{aligned} i_{I,k} = \underline{M}_{ON} & \left[(\alpha_D \underline{I} + \frac{\underline{A}_{ON} \alpha_D^2 T_S}{2}) \underline{x}_{S,SS} + \frac{\underline{B}_{ON} \alpha_D^2 T_S}{2} \underline{u}_I \right] \\ & + \underline{M}_{OFF1} \left[\left(\frac{t_{OFF1} \underline{I}}{T_S} + \frac{\underline{A}_{OFF1} t_{OFF1}^2}{2 T_S} + \underline{A}_{ON} t_{OFF1} \alpha_D \right) \underline{x}_{S,SS} \right. \\ & \quad \left. + \left(\frac{\underline{B}_{OFF1} t_{OFF1}^2}{2 T_S} + \underline{B}_{ON} t_{OFF1} \alpha_D \right) \underline{u}_I \right] \end{aligned} \quad (66)$$

Equation (66) can be rewritten as

$$i_I = f(\underline{x}_{S,SS}, \alpha_D, \underline{v}_I, i_W) \quad (67)$$

Linearizing (66), and then applying the Laplace transformation,

$$I_i(s) = p_{11} V_c(s) + q_{11} A_d(s) + q_{12} V_i(s) + q_{13} I_w(s) \quad (68)$$

where

$$\begin{aligned}
p_{11} = \left. \frac{\partial f}{\partial v_{C,SS}} \right|_* &= \underline{M}_{ON} \left(\underline{A}_D \underline{I} + \frac{\underline{A}_{ON} \underline{A}_D^2 T_S}{2} \right) [1 \ 0]^T \\
&+ \underline{M}_{OFF1} \left(\frac{T_{OFF1} \underline{I}}{T_S} + \frac{\underline{A}_{OFF1} T_{OFF1}^2}{2 T_S} + \underline{A}_{ON} T_{OFF1} \underline{A}_D \right) [1 \ 0]^T \\
&+ \underline{M}_{OFF1} \left[\left(\frac{\underline{I}}{T_S} + \frac{\underline{A}_{OFF1} T_{OFF1}}{T_S} + \underline{A}_{ON} \underline{A}_D \right) \underline{X}_S(kT_S) \right. \\
&\quad \left. + \left(\frac{\underline{B}_{OFF1} T_{OFF1}}{T_S} + \underline{B}_{ON} \underline{A}_D \right) \underline{U}_I \right] \left(\left. \frac{\partial t_{OFF1}}{\partial v_C} \right|_* \right)
\end{aligned} \tag{69a}$$

$$\begin{aligned}
q_{11} = \left. \frac{\partial f}{\partial \alpha_D} \right|_* &= \underline{M}_{ON} \left(\left(\underline{I} + \underline{A}_{ON} \underline{A}_D T_S \right) \underline{X}_S(kT_S) + \underline{B}_{ON} \underline{A}_D T_S \underline{U}_I \right) \\
&+ \underline{M}_{OFF1} \left(\underline{A}_{ON} T_{OFF1} \underline{X}_S(kT_S) + \underline{B}_{ON} T_{OFF1} \underline{U}_I \right) \\
&+ \underline{M}_{OFF1} \left[\left(\frac{\underline{I}}{T_S} + \frac{\underline{A}_{OFF1} T_{OFF1}}{T_S} + \underline{A}_{ON} \underline{A}_D \right) \underline{X}_S(kT_S) \right. \\
&\quad \left. + \left(\frac{\underline{B}_{OFF1} T_{OFF1}}{T_S} + \underline{B}_{ON} \underline{A}_D \right) \underline{U}_I \right] \left(\left. \frac{\partial t_{OFF1}}{\partial \alpha_D} \right|_* \right)
\end{aligned} \tag{69b}$$

$$\begin{aligned}
q_{12} = \left. \frac{\partial f}{\partial v_I} \right|_* &= \left[\frac{\underline{M}_{ON} \underline{B}_{ON} \underline{A}_D^2 T_S}{2} + \frac{\underline{M}_{OFF1} \underline{B}_{OFF1} T_{OFF1}^2}{2 T_S} + \underline{M}_{OFF1} \underline{B}_{ON} T_{OFF1} \underline{A}_D \right] [1 \ 0 \ 0 \ 0]^T \\
&+ \underline{M}_{OFF1} \left[\left(\frac{\underline{I}}{T_S} + \frac{\underline{A}_{OFF1} T_{OFF1}}{T_S} + \underline{A}_{ON} \underline{A}_D \right) \underline{X}_S(kT_S) \right. \\
&\quad \left. + \left(\frac{\underline{B}_{OFF1} T_{OFF1}}{T_S} + \underline{B}_{ON} \underline{A}_D \right) \underline{U}_I \right] \left(\left. \frac{\partial t_{OFF1}}{\partial v_I} \right|_* \right)
\end{aligned} \tag{69c}$$

$$\begin{aligned}
 q_{13} = \frac{\partial f}{\partial i_W} \Big|_* &= \left[\frac{M_{ON} B_{ON} A_D^2 T_S}{2} + \frac{M_{OFF1} B_{OFF1} T_{OFF1}^2}{2 T_S} + M_{OFF1} B_{ON} T_{OFF1} A_D \right] [0 \ 1 \ 0 \ 0]^T \\
 &+ M_{OFF1} \left[\left(\frac{I}{T_S} + \frac{A_{OFF1} T_{OFF1}}{T_S} + A_{ON} A_D \right) \underline{x}_S(k T_S) \right. \\
 &\quad \left. + \left(\frac{B_{OFF1} T_{OFF1}}{T_S} + B_{ON} A_D \right) \underline{u}_I \right] \left(\frac{\partial t_{OFF1}}{\partial i_W} \Big|_* \right)
 \end{aligned}
 \tag{69d}$$

As in the case of the continuous-mmf mode, the frequency dependence of the supply current on the supply voltage is approximated by assigning the poles and zeros of $G_{I_X/V_i}(s)$ as the poles and zeros of $G_{I_i/V_i}(s)$. However, in the case of the discontinuous-mmf mode, $G_{I_X/V_i}(s)$ is identically equal to zero because $i_X(kT_S)$ is always equal to zero. That is, $G_{I_X/V_i}(s)$ is equal to the numerical constant zero. Hence the transfer function $G_{I_i/V_i}(s)$ is also modeled as a proportionality constant without any poles or zeros. Similarly, the transfer function $G_{I_i/I_W}(s)$ is modeled as a numerical constant. Hence the constants given by (69a) through (69d) need no further modification in the modeling of the supply current.

In the case of the continuous-mmf mode, the diode conduction time t_{OFF1} is simply $t_{OFF1} = T_S - t_{ON}$. In the case of the discontinuous-mmf mode, however, t_{OFF1} not only depends on t_{ON} , but also depends on v_I , $v_C(kT_S)$, v_Q , v_D , and i_W . Hence under small-signal perturbation, t_{OFF1} is also a function of not only α_d , but also v_i , v_C , and i_W . As a result, compared to their counterparts in (47), Eqs. (69) have extra terms involving the partial derivatives of t_{OFF1} with respect to the other dynamical variables. The five transfer functions relating the output variables are also listed in Table 4.

Table 4. Five Transfer Functions Describing the Load Voltage and the Supply Current for Discontinuous-Mmf-Mode Operation.

FUNCTION
$G_{V_o/V_c}(s) = -(1 + s r_c C)$
$G_{I_i/V_c}(s) = p_{11}$
$G_{I_i/A_d}(s) = q_{11}$
$G_{I_i/V_i}(s) = q_{12}$
$G_{I_i/I_w}(s) = q_{13}$

Substituting the matrices \underline{A}_{ON} , \underline{A}_{OFF1} , \underline{A}_{OFF2} , \underline{B}_{ON} , \underline{B}_{OFF1} , and \underline{B}_{OFF2} from (19,CVU) through (24,CVU) into (58), and comparing with (59),

$$f_V = -\omega_a v_{C,SS} \left(1 - \frac{\omega_a T_S}{2} + \frac{\rho R_L t_{OFF1}^2}{2L_S T_S} \right) + \frac{\gamma R_L \omega_a (V_I - V_Q) t_{OFF1} t_{ON}}{L_S T_S} \\ - R_L \omega_a i_W \left(1 - \frac{\omega_a T_S}{2} - \frac{\omega_e t_{OFF1}^2}{2T_S} \right) - \frac{R_L \omega_a V_D t_{OFF1}^2}{2L_S T_S} \quad (70, CVU)$$

Unlike operation in the continuous-mmf mode, where $t_{OFF1} = (1 - \alpha_D) T_S$, the diode conduction time t_{OFF1} in the discontinuous-mmf mode depends not only on the duty ratio α_D , but also on the supply voltage V_I , capacitor voltage $v_C(kT_S)$, and load-disturbance current i_W . Although (39,CVU) gives an adequate approximation on the equilibrium diode conduction time T_{OFF1} as a function of the other parameters, it is not sufficient to characterize the small-signal t_{off1} because all parasitic dissipative elements have been deleted in the approximation process. To find out how t_{off1} will vary under small-signal perturbation, the large-signal equation (36,CVU) is re-examined.

$$0 = t_{OFF1}^2 \left(\frac{\rho \omega_a (v_{C,SS} + R_L i_W)}{2L_S} + \frac{\omega_h (\rho v_{C,SS} + V_D)}{2L_S} - \frac{\omega_e \omega_h i_W}{2} \right) \\ + t_{OFF1} \left(\frac{\rho \omega_a t_{ON} (v_{C,SS} + R_L i_W)}{L_S} - \frac{\gamma (V_I - V_Q) \omega_h t_{ON}}{L_S} + \omega_e i_W - \frac{\rho v_{C,SS} + V_D}{L_S} \right) \\ + \left(\frac{\gamma (V_I - V_Q) t_{ON} (2 - \omega_g t_{ON})}{2L_S} \right) \quad (36, CVU)$$

Applying partial differentiation on (36,CVU) with respect to $v_{C,SS}$,

$$\begin{aligned}
0 = & \frac{t_{OFF1}^2 \rho (\omega_a + \omega_h)}{2L_S} + \frac{\rho \omega_a t_{OFF1} t_{ON}}{L_S} - \frac{\rho t_{OFF1}}{L_S} \\
& + 2 t_{OFF1} \left(\frac{\rho \omega_a (V_{C,SS} + R_L I_W)}{2L_S} + \frac{\omega_h (\rho V_{C,SS} + V_D)}{2L_S} - \frac{\omega_e \omega_h I_W}{2} \right) \frac{\partial t_{OFF1}}{\partial V_{C,SS}} \\
& + \left(\frac{\rho \omega_a t_{ON} (V_{C,SS} + R_L I_W)}{L_S} - \frac{\gamma (V_I - V_Q) \omega_h t_{ON}}{L_S} + \omega_e I_W - \frac{\rho V_{C,SS} + V_D}{L_S} \right) \frac{\partial t_{OFF1}}{\partial V_{C,SS}}
\end{aligned}$$

Defining the expression

$$\begin{aligned}
D = & 2 t_{OFF1} \left(\frac{\rho \omega_a (V_Q + R_L I_W)}{2L_S} + \frac{\omega_h (\rho V_Q + V_D)}{2L_S} - \frac{\omega_e \omega_h I_W}{2} \right) \\
& + \left(\frac{\rho \omega_a t_{ON} (V_Q + R_L I_W)}{L_S} - \frac{\gamma (V_I - V_Q) \omega_h t_{ON}}{L_S} - \frac{\rho V_Q + V_D}{L_S} + \omega_e I_W \right) \quad (71, CVU)
\end{aligned}$$

then solving for the partial derivatives gives

$$\left. \frac{\partial t_{OFF1}}{\partial V_{C,SS}} \right|_* = \frac{\rho t_{OFF1}}{DL_S} \left(1 - \omega_a t_{ON} - \frac{(\omega_a + \omega_h) t_{OFF1}}{2} \right) \quad (72a, CVU)$$

All parameters in (71, CVU) and (72a, CVU) are obtained from the algorithms presented in Section 4. Using similar methods,

$$\left. \frac{\partial t_{OFF1}}{\partial \alpha_D} \right|_* = \frac{T_S}{DL_S} \left(t_{OFF1} [\gamma (V_I - V_Q) \omega_h - \rho \omega_a (V_Q + I_W R_L)] - \gamma (V_I - V_Q) (1 - \omega_g A_D T_S) \right) \quad (72b, CVU)$$

$$\left. \frac{\partial t_{OFF1}}{\partial V_I} \right|_* = \frac{\gamma t_{ON}}{DL_S} \left(\omega_h t_{OFF1} - \left(1 - \frac{\omega_g t_{ON}}{2} \right) \right) \quad (72c, CVU)$$

$$\left. \frac{\partial t_{OFF1}}{\partial i_W} \right|_* = - \frac{T_{OFF1}}{DL_S} \left(\frac{T_{OFF1}}{2} (\rho R_L \omega_a - \omega_e \omega_h L_S) + \rho R_L \omega_a A_D T_S + \omega_e L_S \right) \quad (72d, CVU)$$

With the partial derivatives in (72, CVU) derived and evaluated, the partial derivatives of the function f_Y defined in (70, CVU) with respect to the dynamic variables can be found. Defining

$$P_1 = \frac{R_L \omega_a}{T_S} \left(\frac{\gamma(V_I - V_Q) T_{ON} - (\rho V_Q + V_D) T_{OFF1}}{L_S} + \omega_e I_W T_{OFF1} \right) \quad (73, CVU)$$

then

$$a_{11} = \left. \frac{\partial f_Y}{\partial v_{C,SS}} \right|_* = - \omega_a \left(1 - \frac{\omega_a T_S}{2} + \frac{\rho R_L T_{OFF1}^2}{2 L_S T_S} \right) + P_1 \left(\left. \frac{\partial t_{OFF1}}{\partial v_{C,SS}} \right|_* \right) \quad (62a, CVU)$$

$$b_{11} = \left. \frac{\partial f_Y}{\partial \alpha_D} \right|_* = \frac{\gamma R_L \omega_a (V_I - V_Q) T_{OFF1}}{L_S} + P_1 \left(\left. \frac{\partial t_{OFF1}}{\partial \alpha_D} \right|_* \right) \quad (62b, CVU)$$

$$b_{12} = \left. \frac{\partial f_Y}{\partial v_I} \right|_* = \frac{\gamma R_L \omega_a T_{ON} T_{OFF1}}{L_S T_S} + P_1 \left(\left. \frac{\partial t_{OFF1}}{\partial v_I} \right|_* \right) \quad (62c, CVU)$$

$$b_{13} = \left. \frac{\partial f_Y}{\partial i_W} \right|_* = - R_L \omega_a \left(1 - \frac{\omega_a T_S}{2} - \frac{\omega_e T_{OFF1}^2}{2 T_S} \right) + P_1 \left(\left. \frac{\partial t_{OFF1}}{\partial i_W} \right|_* \right) \quad (62d, CVU)$$

After substituting the matrices \underline{A}_{ON} , \underline{A}_{OFF1} , \underline{B}_{ON} , and \underline{B}_{OFF1} from (19, CVU) to (22, CVU) and the matrices \underline{M}_{ON} and \underline{M}_{OFF1} from (50, CVU) and (51, CVU) into (69a) to (69d),

$$p_{11} = 0 \quad (69a, CVU)$$

$$q_{11} = \frac{\gamma^2 (V_I - V_Q) T_{ON}}{L_S} \quad (69b, CVU)$$

$$q_{12} = \frac{\gamma^2 T_{ON}^2}{2L_S T_S} \quad (69c, CVU)$$

$$q_{13} = 0 \quad (69d, CVU)$$

6. CLOSED-LOOP FUNCTIONS OF A REGULATED DC-TO-DC CONVERTER

Although the continuous-mmf mode and the discontinuous-mmf mode have been treated separately in the derivation of the small-signal transfer functions, they can be treated the same now by working with the functions derived in various subsections of Section 5. Under small-signal perturbation, a closed-loop regulated dc-to-dc converter can be represented in block-diagram form as shown in Fig. 13. In the continuous-mmf mode, the functions characterizing the power stage with its load are obtained from the procedures presented in section 5.1. In the discontinuous-mmf mode, the functions $G_{I_X/A_D}(s)$, $G_{I_X/V_i}(s)$, $G_{I_X/I_w}(s)$, and $G_{I_i/I_X}(s)$ are equal to zero, and the remaining functions characterizing the power stage with its load are obtained from the procedures presented in section 5.2. Thus, the block diagram in Fig. 13 can be used to represent a regulated dc-to-dc converter for both continuous-mmf mode or discontinuous-mmf mode operation.

Sometimes the two transfer functions $G_{V_f/V_o}(s)$ and $G_{A_d/V_e}(s)$ are combined into one transfer function

$$G_{A_d/V_o}(s) = [- G_{V_f/V_o}(s)] [G_{A_d/V_e}(s)] \quad (75)$$

where $G_{A_d/V_o}(s)$ is called the transfer function of the controller.

6.1 Loop Gain of a Regulated DC-to-DC Converter

In the block diagram in Fig. 13, there is only one closed loop, which is drawn in a heavy line. By tracing around that heavy-line path, the loop gain $T(s)$ of a regulated converter is found to be :

$$T(s) = [H_{V_f/V_o}(s)] [G_{V_o/V_c}(s)] [G_{V_c/A_d}(s)] [G_{A_d/V_e}(s)]$$

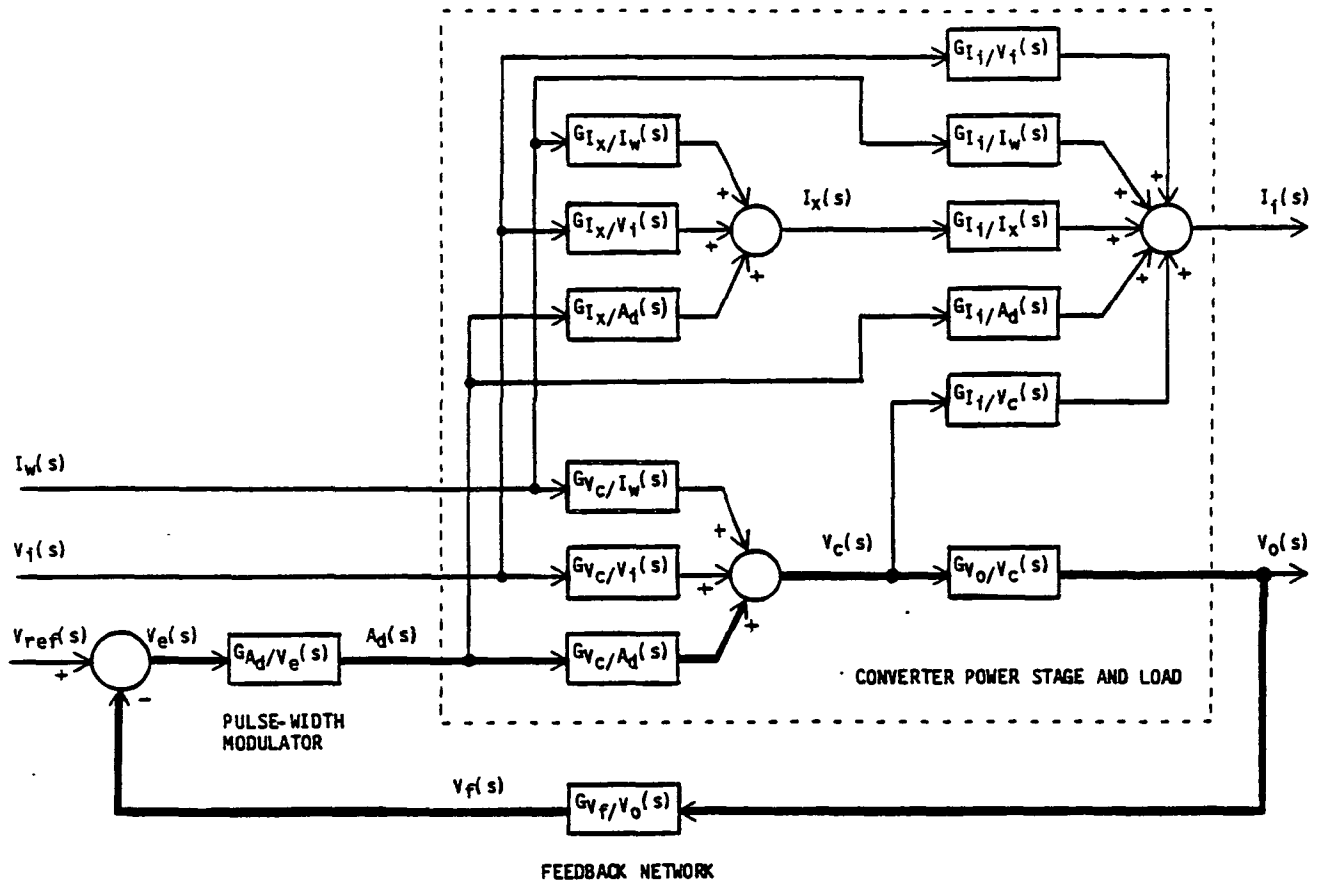


Fig. 13. Block diagram of a regulated dc-to-dc converter operated from a stiff voltage source.

Using (75),

$$T(s) = [-G_{Ad}/V_o(s)] [G_{Vo}/V_c(s)] [G_{Vc}/A_d(s)] \quad (76)$$

where $G_{Vo}/V_c(s)$ and $G_{Vc}/A_d(s)$ are obtained following the procedures explained in Section 5.

6.2 Input Impedance of a Regulated DC-to-DC Converter

To find the input impedance $Z_i(s)$ of a closed-loop regulated dc-to-dc converter, the input admittance function $Y_i(s)$ is derived first.

$$Y_i(s) = \frac{I_i(s)}{V_i(s)} \quad (77)$$

By taking the reciprocal of $Y_i(s)$, the input impedance function $Z_i(s)$ is obtained. Using Mason's gain rule on the block diagram shown in Fig. 13, the input admittance is derived as

$$Y_i(s) = \frac{I_i(s)}{V_i(s)} = \frac{(T_1 + T_2)\Delta + T_3 + T_4 + T_5}{\Delta} \quad (78)$$

where

$$T_1 = [G_{I_i}/V_i(s)] \quad (78a)$$

$$T_2 = [G_{I_i}/I_x(s)] [G_{I_x}/V_i(s)] \quad (78b)$$

$$T_3 = [G_{I_i}/I_x(s)] [G_{I_x}/A_d(s)] [G_{Ad}/V_o(s)] [G_{Vo}/V_c(s)] [G_{Vc}/V_i(s)] \quad (78c)$$

$$T_4 = [G_{I_i}/A_d(s)] [G_{Ad}/V_o(s)] [G_{Vo}/V_c(s)] [G_{Vc}/V_i(s)] \quad (78d)$$

$$T_5 = [G_{I_i}/V_c(s)] [G_{Vc}/V_i(s)] \quad (78e)$$

$$\Delta = 1 + T(s) \quad (78f)$$

and $T(s)$ is defined earlier in (76). Taking the reciprocal of $Y_i(s)$, the input impedance function is

$$Z_i(s) = \frac{1}{Y_i(s)} = \frac{\Delta}{(T_1 + T_2)\Delta + T_3 + T_4 + T_5} \quad (79)$$

6.3 Audio Susceptibility of a Regulated DC-to-DC Converter

The audio susceptibility $S(s)$ is defined as the ratio of per cent change in the load voltage to the per cent change in the supply voltage under small-signal perturbation.

$$S(s) = \frac{V_o(s) / V_o}{V_i(s) / V_i} = \frac{V_i V_o(s)}{V_o V_i(s)}$$

Using Mason's gain rule on the block diagram shown in Fig. 13

$$S(s) = \frac{V_i [G_{V_o/V_c}(s)] [G_{V_c/V_i}(s)]}{V_o \Delta} \quad (80)$$

where Δ is defined in (78f).

6.4 Output Impedance of a Regulated DC-to-DC Converter

The output impedance is defined as $Z_o(s) = V_o(s)/I_w(s)$. Using Mason's gain rule on the block diagram shown in Fig. 13,

$$Z_o(s) = \frac{V_o(s)}{I_w(s)} = \frac{[G_{V_o/V_c}(s)] [G_{V_c/I_w}(s)]}{\Delta} \quad (81)$$

where Δ is defined in (78f).

7. CONCLUSIONS

The modeling of the power stage of the four most commonly used energy-storage dc-to-dc converters -- the voltage step-up, current step-up, single-winding current-or-voltage step-up, and the two-winding current-or-voltage step-up converters -- under small-signal low-frequency perturbation has been presented in the Phase A Report and this Phase B Report. Starting from the time domain, large-signal difference equations relating the state variables at the beginning of each switching cycle are obtained by approximating state transition matrices by second-order Taylor series. For low-frequency disturbances, the derivatives of the state variables can be approximated by the difference equations. For small-signal perturbation around the equilibrium operating point, a set of small-signal differential equations with constant coefficients is obtained from the large-signal differential equations. Applying the Laplace transformation to the small-signal differential equations then yields a set of small-signal transfer functions characterizing the power stage of an energy-storage dc-to-dc converter. Combining these transfer functions with the small-signal transfer functions of the controller gives valuable information such as the loop gain, input impedance, output impedance, and audio susceptibility of the closed-loop regulated dc-to-dc converter.

The procedure for obtaining various small-signal functions of a closed-loop regulated dc-to-dc converter is illustrated, with the current step-up converter on board the Dynamics Explorer Satellite as an example, in Section 8 of the Phase A Report. Following this illustration and the flow charts shown in Figs. 2 of these two reports, various small-signal functions of the voltage step-up, current step-up, single-winding current-or-voltage step-up, and the two-winding current-or-voltage step-up converters can be obtained.

8. REFERENCES

- [1] R.C. Wong, H.A. Owen, Jr., and T.G. Wilson, "Derivation of Linearized Transfer Functions for Switching-Mode Regulators, Phase A — Current Step-Up and Voltage Step-Up Converters," prepared by Center for Solid-State Power Conditioning and Control, Duke University, for NASA Goddard Space Flight Center under Order No. S-71440B, September 29, 1981.

- [2] Y. Yu, R.P. Iwens, F.C. Lee, and L.Y. Inouye, "Development of A Standardized Control Module for DC-DC Converters," NASA Contract Report, NAS3-18918, prepared by TRW Defense and Space System Groups, August 30, 1977.

- [3] R.C. Wong, G.E. Rodriguez, H.A. Owen, Jr., and T.G. Wilson, "Application of Small-Signal Modeling and Measurement Techniques to the Stability Analysis of an Integrated Switching-Mode Power System," IEEE PESC Record - 1980, pp 104-118.

- [4] J.J. D'Azzo and C.H. Houpis, "Linear Control System Analysis and Design : Conventional and Modern," McGraw Hill, 1975, pp 457-460.

APPENDIX A

DEFINITION OF SYMBOLS AND ABBREVIATIONS

α_D	Duty ratio of the transistor switch (the ratio of the transistor conduction time t_{ON} to the switching period T_S), dimensionless
C	Nominal capacitance of the output filter capacitor, farad
CU	Equations applying to the current step-up converter only
CVU	Equations applying to both the single-winding and the two-winding current-or-voltage step-up converters
f_S	Switching frequency, hertz
i_D	Diode current, ampere
i_I	Supply current, ampere
$i_{I,k}$	Average supply current over the k th switching cycle, ampere
i_Q	Transistor current, ampere
$I_{Q,rms}$	Effective value of the transistor current, ampere
i_W	Load disturbance current, ampere
i_X	Current through the ideal inductance in the model of the energy-storage reactor, ampere
L	Nominal inductance of the single-winding reactor, henry
L_S	Nominal secondary inductance of the two-winding reactor, henry
N_p	Number of turns in the primary winding of the two-winding reactor, dimensionless
N_S	Number of turns in the secondary winding of the two-winding reactor, dimensionless
P_Q	Power loss in the transistor switch, watt
P_R	Power loss in the transistor switch due to an equivalent resistance, watt
P_V	Power loss in the transistor switch due to the saturation voltage drop, watt
r_C	Equivalent series resistance (ESR) of the filter capacitor, ohm

r_D	Equivalent diode resistance, ohm
r_D'	Dynamic resistance of the diode as measured from a curve tracer, ohm
R_L	Load resistance, ohm
r_Q	Equivalent transistor resistance, ohm
r_Q'	Saturation resistance of the transistor as measured from a curve tracer, ohm
r_p	Primary winding resistance of the two-winding reactor, ohm
r_s	Secondary winding resistance of the two-winding reactor, ohm
r_x	Winding resistance of the single-winding reactor, ohm
SCVU	Single-winding current-or-voltage step-up converter
TCVU	Two-winding current-or-voltage step-up converter
\underline{u}_I	input vector, equal to $[v_I \ i_W \ V_Q \ V_D]^T$
v_C	Voltage across the ideal capacitance of the filter capacitor, volt
v_D	Voltage across the diode switch, volt
V_D	Break-point voltage of the diode, volt
v_E	Error voltage of the error comparator, volt
v_F	Feedback voltage of the feedback network, volt
v_I	Supply voltage, volt
v_O	Load voltage, volt
v_Q	Voltage across the transistor, volt
V_Q	Saturation voltage of the transistor, volt
V_{REF}	Reference voltage for establishing the desired output voltage, volt
VU	Equations applying to the voltage step-up converter only
\underline{x}_S	state vector, equal to $[v_C \ i_X]^T$
$\underline{x}_{S,SS}$	Stroboscopic value of the state vector at the beginning of each switching cycle
γ	Secondary-to-primary turn ratio, equal to N_S/N_P , dimensionless

APPENDIX B

EQUATIONS DEFINING THE CONSTANTS AND THE COEFFICIENTS
IN THE TRANSFER FUNCTIONS

For SCVU, let $\gamma = 1$, $L_S = L$, $r_p = r_X$, and $r_S = r_X$.

$$\rho = \frac{R_L}{r_C + R_L} \quad (3)$$

$$\omega_a = \frac{1}{C(r_C + R_L)} \quad (4)$$

$$\gamma = \frac{N_S}{N_P} \quad (5)$$

$$\omega_e = \frac{\rho r_C}{L_S} \quad (6)$$

$$\omega_g = \frac{\gamma^2 (r_p + r_Q)}{L_S} \quad (7)$$

$$\omega_h = \frac{r_S + r_D + \rho r_C}{L_S} \quad (8)$$

$$\begin{aligned} 0 = & -\omega_a V_C (kT_S) \left(1 - \frac{\omega_a T_S}{2} + \frac{\rho R_L (1-A_D)^2 T_S}{2L_S} \right) \\ & + I_X (kT_S) R_L \omega_a (1-A_D) \left(1 - \omega_g A_D T_S - \frac{(\omega_a + \omega_h)(1-A_D) T_S}{2} \right) \\ & + \frac{\gamma V_I R_L \omega_a (1-A_D) A_D T_S}{L_S} - I_W R_L \omega_a \left(1 - \frac{\omega_a T_S}{2} - \frac{\omega_e (1-A_D)^2 T_S}{2} \right) \\ & - \frac{\gamma V_Q R_L \omega_a (1-A_D) A_D T_S}{L_S} - \frac{V_D R_L \omega_a (1-A_D)^2 T_S}{2L_S} \end{aligned} \quad (28, CVU)$$

$$A_D = \frac{V_O + V_D}{\gamma(V_I - V_Q) + V_O + V_D} \quad (30, CVU)$$

$$I_X(kT_S) = \frac{1}{(1-A_D)} \left(\frac{V_0}{R_L} + I_W \right) - \frac{\gamma(V_I - V_Q)A_D T_S}{2L_S} \quad (31, CVU)$$

$$\begin{aligned} 0 = A_D^2 T_S \left[\frac{\rho(\omega_h \omega_a) V_0}{2L_S} - \frac{I_X(kT_S)}{2} \left(\frac{\rho R_L \omega_a}{L_S} - (\omega_g - \omega_h)^2 \right) \right. \\ \left. - \frac{I_W}{2} \left(\frac{\rho R_L \omega_a}{L_S} + \omega_e \omega_h \right) - \frac{\gamma(V_I - V_Q)(\omega_g - 2\omega_h)}{2L_S} + \frac{V_D \omega_h}{2L_S} \right] \\ + A_D \left[(1 - \omega_h T_S) \left(\frac{\rho V_0 + V_D + \gamma(V_I - V_Q)}{L_S} - \omega_e I_W + (\omega_h \omega_g) I_X(kT_S) \right) \right. \\ \left. + \frac{I_X(kT_S) \rho R_L \omega_a T_S}{L_S} \right] \\ + \left[\frac{(2 - \omega_h T_S)}{2} \left(- \frac{V_D + \rho V_0}{L_S} - \omega_h I_X(kT_S) + \omega_e I_W \right) \right. \\ \left. + \frac{\rho \omega_a T_S (V_0 - R_L I_X(kT_S) + R_L I_W)}{2L_S} \right] \quad (32, CVU) \end{aligned}$$

$$\begin{aligned} 0 = T_{OFF1}^2 \left(\frac{\rho \omega_a (V_0 + R_L I_W)}{2L_S} + \frac{\omega_h (\rho V_0 + V_D)}{2L_S} - \frac{\omega_e \omega_h I_W}{2} \right) \\ + T_{OFF1} \left(\frac{\rho \omega_a T_{ON} (V_0 + R_L I_W)}{L_S} - \frac{\gamma(V_I - V_Q) \omega_h T_{ON}}{L_S} - \frac{\rho V_0 + V_D}{L_S} + \omega_e I_W \right) \\ + \left(\frac{\gamma(V_I - V_Q) T_{ON} (2 - \omega_g T_{ON})}{2L_S} \right) \quad (38, CVU) \end{aligned}$$

$$T_{OFF1} = \frac{\gamma(V_I - V_Q) T_{ON}}{V_0 + V_D} = \frac{\gamma(V_I - V_Q) A_D T_S}{V_0 + V_D} \quad (39, CVU)$$

$$A_D = \sqrt{\frac{2L_S (V_0 + R_L I_W) (V_0 + V_D)}{\gamma^2 R_L T_S (V_I - V_Q)^2}} \quad (40, CVU)$$

$$0 = A_D \left(\frac{\gamma(V_I - V_Q) R_L T_{OFF1}}{L_S} \right) + \left[-V_O \left(1 - \frac{\omega_a T_S}{2} + \frac{\rho R_L T_{OFF1}^2}{2L_S T_S} \right) - \frac{V_D R_L T_{OFF1}^2}{2L_S T_S} - R_L I_W \left(1 - \frac{\omega_a T_S}{2} - \frac{\omega_e T_{OFF1}^2}{2T_S} \right) \right] \quad (41, CVU)$$

$$a_{11} = -\omega_a \left(1 - \frac{\omega_a T_S}{2} + \frac{\rho R_L (1-A_D)^2 T_S}{2L_S} \right) \quad (46a, CVU)$$

$$a_{12} = R_L \omega_a \left((1-A_D) - \omega_g (1-A_D) A_D T_S - \frac{(\omega_a + \omega_h)(1-A_D)^2 T_S}{2} \right) \quad (46b, CVU)$$

$$b_{11} = \frac{R_L \omega_a \rho V_O (1-A_D) T_S}{L_S} - R_L \omega_a I_X (k T_S) \left(1 + \omega_g (1-2A_D) T_S - (\omega_a + \omega_h)(1-A_D) T_S \right) - R_L \omega_a I_W \omega_e (1-A_D) T_S + \frac{\gamma R_L \omega_a (V_I - V_Q)(1-2A_D) T_S}{L_S} + \frac{R_L \omega_a V_D (1-A_D) T_S}{L_S} \quad (46c, CVU)$$

$$b_{12} = \frac{\gamma R_L \omega_a (1-A_D) A_D T_S}{L_S} \quad (46d, CVU)$$

$$b_{13} = -R_L \omega_a \left(1 - \frac{\omega_a T_S}{2} - \frac{\omega_e (1-A_D)^2 T_S}{2} \right) \quad (46e, CVU)$$

$$a_{21} = -\frac{\rho}{L_S} \left((1-A_D) - \frac{\omega_a (1-A_D)^2 T_S}{2} - \frac{\omega_h (1-A_D)^2 T_S}{2} \right) \quad (46f, CVU)$$

$$a_{22} = -\left(\omega_g A_D + \omega_h (1-A_D) - \frac{(\omega_g A_D + \omega_h (1-A_D))^2 T_S}{2} + \frac{\rho R_L \omega_a (1-A_D)^2 T_S}{2L_S} \right) \quad (46g, CVU)$$

$$\begin{aligned}
b_{21} = & \frac{\rho V_0}{L_S} (1 - \omega_a A_D T_S - \omega_h (1 - A_D) T_S) \\
& - I_X (k T_S) (\omega_g - \omega_h - (\omega_g - \omega_h) (\omega_g A_D + \omega_h (1 - A_D)) T_S - \frac{\rho R_L \omega_a (1 - A_D) T_S}{L_S}) \\
& - I_W (\omega_e + \frac{\rho R_L \omega_a A_D T_S}{L_S} - \omega_e \omega_h (1 - A_D) T_S) + \frac{V_D}{L_S} (1 - \omega_h (1 - A_D) T_S) \\
& + \frac{\gamma (V_I - V_Q)}{L_S} (1 - \omega_h (1 - 2 A_D) T_S - \omega_g A_D T_S) \quad (46 h, CVU)
\end{aligned}$$

$$b_{22} = \frac{\gamma}{L_S} (A_D - \frac{\omega_g A_D^2 T_S}{2} - \omega_h (1 - A_D) A_D T_S) \quad (46 i, CVU)$$

$$b_{23} = (\omega_e (1 - A_D) + \frac{\rho R_L \omega_a (1 - A_D^2) T_S}{2 L_S} - \frac{\omega_e \omega_h (1 - A_D)^2 T_S}{2}) \quad (46 j, CVU)$$

$$p_{11} = 0 \quad (57 a, CVU)$$

$$p_{12} = \gamma A_D (1 - \frac{\omega_g A_D T_S}{2}) \quad (57 b, CVU)$$

$$q_{11} = \gamma I_X (k T_S) (1 - A_D \omega_g T_S) + \frac{\gamma^2 (V_I - V_Q) A_D T_S}{L_S} \quad (57 c, CVU)$$

$$q_{12} = \frac{\gamma^2 A_D^2 T_S}{2 L_S} \quad (57 d, CVU)$$

$$q_{13} = 0 \quad (57 e, CVU)$$

$$a_{11} = \left. \frac{\partial f_V}{\partial v_{C,SS}} \right|_* = -\omega_a (1 - \frac{\omega_a T_S}{2} + \frac{\rho R_L T_{OFF1}^2}{2 L_S T_S}) + p_1 \left(\left. \frac{\partial t_{OFF1}}{\partial v_{C,SS}} \right|_* \right) \quad (62 a, CVU)$$

$$b_{11} = \left. \frac{\partial f_V}{\partial \alpha_D} \right|_* = \frac{\gamma R_L \omega_a (V_I - V_Q) T_{OFF1}}{L_S} + p_1 \left(\left. \frac{\partial t_{OFF1}}{\partial \alpha_D} \right|_* \right) \quad (62 b, CVU)$$

$$b_{12} = \left. \frac{\partial f_V}{\partial v_I} \right|_* = \frac{\gamma R_L \omega_a T_{ON} T_{OFF1}}{L_S T_S} + P_1 \left(\left. \frac{\partial t_{OFF1}}{\partial v_I} \right|_* \right) \quad (62c, CVU)$$

$$b_{13} = \left. \frac{\partial f_V}{\partial i_W} \right|_* = - R_L \omega_a \left(1 - \frac{\omega_a T_S}{2} - \frac{\omega_e T_{OFF1}^2}{2 T_S} \right) + P_1 \left(\left. \frac{\partial t_{OFF1}}{\partial i_W} \right|_* \right) \quad (62d, CVU)$$

$$p_{11} = 0 \quad (69a, CVU)$$

$$q_{11} = \frac{\gamma^2 (V_I - V_Q) T_{ON}}{L_S} \quad (69b, CVU)$$

$$q_{12} = \frac{\gamma^2 T_{ON}^2}{2 L_S T_S} \quad (69c, CVU)$$

$$q_{13} = 0 \quad (69d, CVU)$$

$$D = 2 T_{OFF1} \left(\frac{\rho \omega_a (V_Q + R_L I_W)}{2 L_S} + \frac{\omega_h (\rho V_Q + V_D)}{2 L_S} - \frac{\omega_e \omega_h I_W}{2} \right) \\ + \left(\frac{\rho \omega_a T_{ON} (V_Q + R_L I_W)}{L_S} - \frac{\gamma (V_I - V_Q) \omega_h T_{ON}}{L_S} - \frac{\rho V_Q + V_D}{L_S} + \omega_e I_W \right) \quad (71, CVU)$$

$$\left. \frac{\partial t_{OFF1}}{\partial v_{C,SS}} \right|_* = \frac{\rho T_{OFF1}}{D L_S} \left(1 - \omega_a T_{ON} - \frac{(\omega_a + \omega_h) T_{OFF1}}{2} \right) \quad (72a, CVU)$$

$$\left. \frac{\partial t_{OFF1}}{\partial \alpha_D} \right|_* = \frac{T_S}{D L_S} \left(T_{OFF1} [\gamma (V_I - V_Q) \omega_h - \rho \omega_a (V_Q + I_W R_L)] - \gamma (V_I - V_Q) (1 - \omega_g A_D T_S) \right) \quad (72b, CVU)$$

$$\left. \frac{\partial t_{OFF1}}{\partial v_I} \right|_* = \frac{\gamma T_{ON}}{D L_S} \left(\omega_h T_{OFF1} - \left(1 - \frac{\omega_g T_{ON}}{2} \right) \right) \quad (72c, CVU)$$

$$\left. \frac{\partial t_{OFF1}}{\partial i_W} \right|_* = - \frac{T_{OFF1}}{DL_S} \left(\frac{T_{OFF1}}{2} (\rho R_{L\omega a} - \omega_e \omega_h L_S) + \rho R_{L\omega a} A_D T_S + \omega_e L_S \right) \quad (72d, CVU)$$

$$P_1 = \frac{R_{L\omega a}}{T_S} \left(\frac{\gamma(V_I - V_Q) T_{ON} - (\rho V_Q + V_D) T_{OFF1}}{L_S} + \omega_e I_W T_{OFF1} \right) \quad (73, CVU)$$